Chirality dependence in charge and heat transport in thermal QCD

Pushpa Panday[*] and Binoy Krishna Patra[†]

Department of Physics, Indian Institute of Technology Roorkee, Roorkee 247667, India

(Received 10 February 2022; revised 26 May 2022; accepted 26 May 2022; published 15 June 2022)

As the strength of the magnetic field (B) becomes weak, novel phenomena, similar to the Hall effect in condensed matter physics, emerges both in charge and heat transport in a thermal QCD medium with a finite quark chemical potential (μ). So we have calculated the transport coefficients in a kinetic theory within a quasiparticle framework, wherein we compute the effective mass of quarks for the aforesaid medium in a weak magnetic field (B) limit ($|eB| \ll T^2$; T is temperature) by the perturbative thermal QCD up to one loop, which depends on T and B differently to left-handed (L) and right-handed (R) chiral modes of quarks, lifting the prevalent degeneracy in L and R modes in strong magnetic field limit ($|eB| \gg T^2$). Another implication of weak B is that the transport coefficients assume a tensorial structure: The diagonal elements represent the usual (electrical and thermal) conductivities (σ_{Ohmic} and κ_0 as the coefficients of charge and heat transport, respectively) and the off-diagonal elements denote their Hall counterparts (σ_{Hall} and κ_1, respectively). It is found in charge transport that the magnetic field acts on L and R modes of the Ohmic part of electrical conductivity in an opposite manner, viz. σ_{Ohmic} for L mode decreases and for R mode, increases with B whereas the Hall-part σ_{Hall} for both L and R modes always increases with B. In heat transport too, the effect of the magnetic field on the usual thermal conductivity (κ_0) and Hall-type coefficient (κ_1) in both modes is identical to the above-mentioned effect of B on charge transport coefficients. We have then derived some coefficients from the above transport coefficients, *namely* Knudsen number (Ω is the ratio of the mean-free path to the length scale of the system) and Lorenz number in Wiedemann-Franz law. The effect of B on Ω either with κ_0 or with κ_1 for both modes is identical to the behavior of κ_0 and κ_1 with B. The value of Ω is always less than unity for the entire temperature range, validating our calculations. Lorenz number ($\kappa_0/\sigma_{\text{Ohmic}}T$) and Hall-Lorenz number ($\kappa_1/\sigma_{\text{Hall}}T$) for L mode increases and for R mode decreases with magnetic field. It also does not remain constant with temperature hence violating the Wiedemann-Franz law.

DOI: 10.1103/PhysRevD.105.116009

I. INTRODUCTION

Quark-gluon plasma (QGP) is the deconfined phase of quarks and gluons which is believed to have existed in the early universe, about 10^{-5} sec after the cosmic big bang and at the core of superdense stars such as neutron stars and quark stars. Experiments at European Council for Nuclear Research, Relativistic Heavy Ion Collider, Brookhaven National Laboratory and Large Hadron Collider (LHC) have been successful in creating QGP in colliders [1]. It is also established that a magnetic field, whose magnitude varies from $|eB| = 0.1m_\pi^2$ for Super Proton Synchrotron energy to $|eB| = 15m_\pi^2$ for LHC, is also produced during noncentral heavy ion collisions [2–4]. The strength of this magnetic field is strong during the initial stages of QGP but it decays very fast with time. The lifetime of magnetic field in a charged medium, however, gets enhanced due to the charge properties of the medium [5–8]. As the nonvanishing magnetic field can affect the evolution of strongly interacting matter significantly [9–16], therefore the detailed study of its effects on transport phenomena [17,18], thermodynamical behavior [19,20] of quark-gluon plasma, dilepton production from QGP [21–23] has been done. Further, the bulk evolution of QGP matter via relativistic hydrodynamics has been described successfully, which gave satisfactorily the collective flow of the created matter detected in experiments [24–26]. The small ratio of shear viscosity to the entropy density (η/s) of strongly interacting plasma agrees well with the lower bound of $\eta/s = \frac{1}{4\pi}$, where $\hbar = 1, k_B = 1$, obtained using AdS/CFT correspondence [27] hence, validates the use of hydrodynamical model of QGP [28–32]. The evolution of QGP after heavy-ion collisions can be studied using relativistic hydrodynamics where transport coefficients serve as input parameters.

We study the charge and heat transport coefficients which also play an important role in the hydrodynamical description of strongly interacting matter [33–35]. The topological effects induced by the magnetic field can be

[*]pushpa@ph.iitr.ac.in
[†]binoy@ph.iitr.ac.in

quantified using electrical conductivity and play a crucial role in the study of the chiral magnetic effect [36], which is a signature of CP violation in the strong interaction. Dilepton and photon production rates are used to probe the thermalized strongly interacting matter because they hardly interact with the hadrons in the region of hot and dense matter and hence carry information about the early stage of heavy ion collisions. Electrical conductivity (σ_{el}) can be used for phenomenological studies of heavy ion collisions [37]. Another key transport coefficient is thermal conductivity of the QGP medium, which measures the transport of heat due to temperature gradient in the medium. The hydrodynamical equilibrium of the system can be determined using Knudsen number, which is the ratio of mean-free path to the characteristic length of the medium. The mean-free path (λ) is related to the thermal conductivity (κ) as $\lambda = 3\kappa/(\mathrm{v}C_v)$, where v is the relative velocity of quark and C_v is the specific heat at constant volume. Further, the relative behavior of κ and σ_{el} can be understood in terms of Wiedemann-Franz law, which states that ratio, $\kappa/\sigma_{\mathrm{el}}$, of the thermal to electrical conductivity is directly proportional to the temperature, with proportionality constant being roughly the same for all metals. The ratio $\kappa/(\sigma_{\mathrm{el}}T)$ is known as Lorenz number (L), which is independent of temperature and depends on fundamental constants for all metals [38]. However, the violation of Wiedemann-Franz law has been observed in many systems, such as hydrodynamic electron liquid [39], high temperature superconductors [40], Luttinger liquid [41], strongly interacting QGP medium [42] and hot hadronic matter [43]. Hence, it would be interesting to study the Wiedemann-Franz law in our system of interest.

In the present work, we have explored the effect of (a) weak magnetic field and (b) baryon asymmetry, in charge and heat transport phenomena. The weak and strong magnetic field limit can be understood from the relativistic dispersion relation of a fermion of mass m in a uniform magnetic field ($\mathbf{B} = B\hat{z}$):

$$E_n^2 = p_z^2 + m^2 + 2nqB. \tag{1}$$

Here, $n = 0, 1, 2, \ldots$ denotes the Landau levels. The probability of fermions getting thermally excited to higher Landau levels is exponentially suppressed as $\exp(\frac{-\sqrt{qB}}{T})$ [44]. (i) In the strong magnetic field limit, $\sqrt{qB} \gg T$, so the fermions occupy only the lowest Landau level ($n = 0$). This is known as LLL approximation. (ii) If $\sqrt{qB} \ll T$, then fermions can occupy higher Landau levels. This implies that the thermal energy is much larger than the energy level spacing ($\sim\sqrt{qB}$) so that T can excite fermions into the excited states, which justifies calling the condition $qB \ll T^2$, the weak magnetic field limit. The transport coefficients can be calculated in strong and weak magnetic field using different approaches/models, viz. Nambu-Jona-Lasinio model [45–47], Chapmann-Enskog approximation [48–50], the correlator technique using Green-Kubo formula [51–54], effective fugacity model [55–58], lattice simulation [59–61]. However, we have used the kinetic theory approach by solving the relativistic Boltzmann transport equation. The calculation of transport coefficients using kinetic theory has been done [18,62,63] in the presence of strong magnetic field ($q_fB \gg T^2, m_f^2$), where q_f and m_f are the electric charge and mass of quark for fth flavor. In a strongly magnetized medium, the motion of charged particle is restricted to the $1+1$-dimensional Landau level dynamics, where quark momentum is along the direction of magnetic field. In the presence of a weak magnetic field, however, temperature is the dominant energy scale ($T^2 > q_fB > m_f^2$) and the effect of magnetic field comes through the cyclotron frequency (ω_c). In contrast to the case of a strong background magnetic field, motion of charges is no longer restricted to be along the direction of magnetic field, which gives rise to "transverse" responses. This can also be understood via the tensor structure of the transport coefficients at the two magnetic field strength regimes. In the case of strong magnetic field, the coefficient matrix is diagonal, whereas in the presence of a weak magnetic field, off-diagonal elements also manifest. The off diagonal elements are represented by σ_{Hall} and κ_1 in the case of electrical and thermal conductivities respectively. This is corroborated by the fact that there is no σ_{Hall} and κ_1 in the case of strong magnetic field. Furthermore, σ_{Hall} and κ_1 vanish even in the presence of a weak magnetic field if the chemical potential, μ, is zero [64]. The role of interaction among partons is incorporated using a quasiparticle description of partons, where vacuum masses of partons are replaced by medium generated masses. The medium generated mass is calculated from the pole of propagator, obtained through perturbative thermal QCD in the presence of background weak magnetic field. In some previous studies, authors have incorporated the pure thermal medium mass of quarks in the computation of transport coefficients [64,65], whereas we have used the thermally generated mass with magnetic field correction. The dispersion relation of quasiparticles in the weak magnetic field gives rise to four collective modes, two from left-handed and two from right-handed modes. Various properties of dispersion relation have been discussed in [66,67]. The degeneracy in left- and right-handed chiral modes of quarks is lifted due to their different mass in the presence of weak magnetic field, which is in contrast to the case of strong magnetic field. The system can be either in left-handed mode or right-handed mode, hence the medium generated masses for left- and right-handed chiral modes of quarks have been taken into account separately for the estimation of transport coefficients under both modes. We further studied the physical behavior of the system using the aforementioned transport coefficients via Knudsen number and Wiedemann-Franz law for both modes separately.

The paper is organized as follows: in Sec. II, we discuss the quasiparticle model of partons and hence evaluate the medium generated mass. We use this mass as an input to incorporate the interactions among partons, in our calculation of transport coefficients. In Secs. III and IV, we discuss the computation of charge and heat transport coefficients using kinetic theory within the relaxation time approximation. In Sec. V, we present and discuss the results for Ohmic and Hall conductivity, thermal and Hall-type thermal conductivity, Knudsen number and Wiedemann-Franz law. Finally, we conclude our work in Sec. VI.

II. QUASIPARTICLE MODEL FOR HOT AND DENSE QCD MATTER

At asymptotically high temperature, a system of quarks and gluons can be treated as an ideal gas due to asymptotic freedom. The interaction among quasiquarks and quasigluons can be incorporated through medium dependent mass of quasiparticles which can be evaluated using one-loop perturbative thermal QCD. In pure thermal medium at finite quark chemical potential (μ), the thermally generated mass for quarks and gluons is obtained to be as [68]

$$m_{th}^2 = \frac{1}{8}g^2 C_F\left(T^2 + \frac{\mu^2}{\pi^2}\right),$$
$$m_g^2 = \frac{1}{6}g^2 T^2\left(C_A + \frac{1}{2}N_f\right), \tag{2}$$

respectively, where $C_F = (N_c^2 - 1)/2N_C = \frac{4}{3}$ for $N_C = 3$, $C_A (C_A = 3)$ is the group factor, N_f is the number of flavor, g is the QCD coupling constant with $g^2 = 4\pi\alpha_s$, where α_s is the one-loop running coupling constant, which runs with temperature as [69]

$$\alpha_s(\Lambda^2) = \frac{1}{b_1 \ln\left(\frac{\Lambda^2}{\Lambda_{\overline{MS}}^2}\right)}, \tag{3}$$

where $b_1 = (11N_c - 2N_f)/12\pi$ and $\Lambda_{\overline{\rm MS}} = 0.176$ GeV. The renormalization scale for quarks and gluons is chosen to be $\Lambda_q = 2\pi\sqrt{T^2 + \mu^2/\pi^2}$ and $\Lambda_g = 2\pi T$ respectively. Further, the dispersion relation of fermions in pure thermal medium ($B = 0$) in the low ($p \ll m_{th}$) momentum and high momentum ($p \gg m_{th}$) limit are given as [68,70]

$$\omega_+(p) = m_{th} + \frac{p}{3}; \qquad p \ll m_{th} \tag{4}$$

$$\omega_+(p) = p + \frac{m_{th}^2}{p}; \qquad p \gg m_{th}. \tag{5}$$

As we can see, the thermal mass in both the low and high momentum limits is of the same order, $m_{th} \sim gT$.

The effective quark mass for fth flavor can be written as [71]

$$m_f^2 = m_{f0}^2 + \sqrt{2}m_{f0}m_{f,th} + m_{f,th}^2, \tag{6}$$

where m_{f0} and $m_{f,th}$ are the current quark mass and thermal mass for fth flavor respectively. In presence of magnetic field, the one-loop running coupling constant, which runs with temperature and magnetic field, is given by [69]

$$\alpha_s(\Lambda^2, |eB|) = \frac{\alpha_s(\Lambda^2)}{1 + b_1\alpha_s(\Lambda^2)\ln\left(\frac{\Lambda^2}{\Lambda^2 + |eB|}\right)}. \tag{7}$$

The effective quark mass in the presence of magnetic field can be generalized to

$$m_f^2 = m_{f0}^2 + \sqrt{2}m_{f0}m_{fth,B} + m_{fth,B}^2, \tag{8}$$

where $m_{fth,B}$ can be obtained by taking the static limit of the denominator of the dressed quark propagator in the magnetic field. The inverse of the dressed quark propagator using the Schwinger-Dyson equation can be written as

$$S^{*-1}(P) = S^{-1}(P) - \Sigma(P)$$
$$= \not{P} - \Sigma(P), \tag{9}$$

where $S^{-1}(P)$ is the bare inverse propagator and $\Sigma(P)$ is the quark self-energy. So, to calculate the effective quark propagator in the presence of magnetic field at finite temperature, we need to evaluate the quark self-energy as shown in Fig. 1. The quark propagator in the presence of a background magnetic field following the Schwinger formalism can be written in terms of the Laguerre polynomial ($L_l(2\alpha)$) [72]

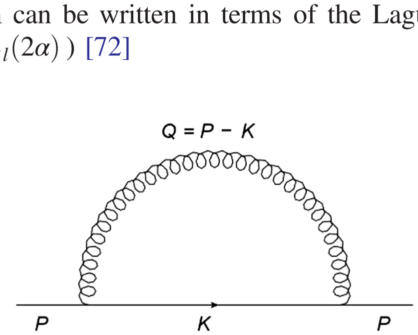

FIG. 1. One-loop quark self-energy in hot and magnetized medium.

$$iS(K) = \sum_{l=0}^{\infty} \frac{-id_l(\alpha)D + d'_l(\alpha)\bar{D}}{k_L^2 + 2l|q_fB|} + \frac{i\gamma.k_\perp}{k_\perp^2}, \quad (10)$$

where q_f is the absolute charge of fth flavor, $l = 0, 1, 2, \ldots$ are the Landau levels, $||$ and $\perp$ are the parallel and perpendicular components of momentum, respectively, with respect to direction of magnetic field, $\alpha = k_\perp^2/|q_fB|$, $k_L^2 = m_{f0}^2 - k_{||}^2$ and $d_l(\alpha), d'_l(\alpha), D, \bar{D}$ are given as [73]

$$\begin{aligned} d_l(\alpha) &= (-1)^l e^{-\alpha} C_l(2\alpha), \\ d'_l(\alpha) &= \frac{\partial d_l}{\partial \alpha}, \\ D &= (m_{f0} + \gamma.k_{||}) + \gamma.k_\perp \left(\frac{m_{f0}^2 - k_{||}^2}{k_\perp^2} \right), \\ \bar{D} &= \gamma_1\gamma_2(m_{f0} + \gamma.k_{||}), \end{aligned} \quad (11)$$

with $C_l(2\alpha) = L_l(2\alpha) - L_{l-1}(2\alpha)$. In the weak field limit, the quark propagator can be reorganized in a power series of magnetic field ($\mathbf{q_f B}$) as

$$iS(K) = \frac{i(\not{K} + m_{f0})}{K^2 - m_{f0}^2} - \frac{\gamma_1\gamma_2(\gamma.K_{||} + m_{f0})}{(K^2 - m_{f0}^2)^2}(q_fB), \quad (12)$$

where the first term in Eq. (12) is the free fermion propagator and the second term is the $\mathcal{O}(q_fB)$ correction to it. Neglecting the current quark mass under the limit ($m_{f0}^2 < q_fB < T^2$) in the numerator and using the following metric tensor in Eq. (12),

$$\begin{aligned} &g^{\mu\nu} = g_{||}^{\mu\nu} + g_\perp^{\mu\nu}; \\ &g_{||}^{\mu\nu} = \mathrm{diag}(1,0,0,-1); \qquad g_\perp^{\mu\nu} = \mathrm{diag}(0,-1,-1,0); \\ &p^\mu = p_{||}^\mu + p_\perp^\mu; \qquad p_{||}^\mu = (p^0,0,0,p^3); \\ &p_\perp^\mu = (0,p^1,p^2,0); \qquad \not{p} = \gamma^\mu p_\mu = \not{p}_{||} + \not{p}_\perp; \\ &\not{p}_{||} = \gamma^0 p_0 - \gamma^3 p^3; \qquad \not{p}_\perp = \gamma^1 p^1 + \gamma^2 p^2, \end{aligned} \quad (13)$$

with

$$i\gamma_1\gamma_2\not{K}_{||} = -\gamma_5[(K.b)\not{u} - (K.u)\not{b}], \quad (14)$$

we obtain the quark propagator in the presence of a magnetic field at finite temperature as

$$iS(K) = \frac{i\not{K}}{K^2 - m_{f0}^2} - \frac{i\gamma_5[(K.b)\not{u} - (K.u)\not{b}]}{(K^2 - m_{f0}^2)^2}(q_fB), \quad (15)$$

where $u^\mu = (1,0,0,0)$ denotes the local rest frame of the heat bath. Introduction of a particular frame of reference breaks the Lorentz symmetry of the system. Similarly, $b^\mu = (0,0,0,1)$ denotes the preferred direction of the magnetic field in our system which then breaks the rotational symmetry of the system. Using the quark propagator (15), the one-loop quark self-energy up to $\mathcal{O}(q_fB)$ in hot and weakly magnetized medium can be written as

$$\Sigma(P) = g^2 C_F T \sum_n \int \frac{d^3k}{(2\pi)^3} \gamma_\mu \left(\frac{\not{K}}{(K^2 - m_{f0}^2)} - \frac{\gamma_5[(K.b)\not{u} - (K.u)\not{b}]}{(K^2 - m_{f0}^2)^2}(q_fB) \right) \gamma^\mu \frac{1}{(P-K)^2}, \quad (16)$$

where T is the temperature of the system and $g^2 = 4\pi\alpha_s(\Lambda^2, |eB|)$. The first term is the thermal medium contribution (Σ_0) whereas the second one is with magnetic field correction term (Σ_1).

The general covariant structure of quark self-energy at finite temperature and magnetic field can be written as [66]

$$\Sigma(P) = -\mathcal{A}\not{P} - \mathcal{B}\not{u} - \mathcal{C}\gamma_5\not{u} - \mathcal{D}\gamma_5\not{b}, \quad (17)$$

where $\mathcal{A}$, $\mathcal{B}$, $\mathcal{C}$, $\mathcal{D}$ are the structure functions. Using Eqs. (16) and (17), the general form of these structure functions is obtained as

$$\mathcal{A}(p_0, p_\perp, p_z) = \frac{1}{4} \frac{\mathrm{Tr}(\Sigma(P)\not{P}) - (P.u)\mathrm{Tr}(\Sigma(P)\not{u})}{(P.u)^2 - P^2}, \quad (18)$$

$$\mathcal{B}(p_0, p_\perp, p_z) = \frac{1}{4} \frac{(-P.u)\mathrm{Tr}(\Sigma(P)\not{P}) + P^2\mathrm{Tr}(\Sigma(P)\not{u})}{(P.u)^2 - P^2}, \quad (19)$$

$$\mathcal{C}(p_0, p_\perp, p_z) = -\frac{1}{4}\mathrm{Tr}(\gamma_5\Sigma(P)\not{u}), \quad (20)$$

$$\mathcal{D}(p_0, p_\perp, p_z) = \frac{1}{4}\mathrm{Tr}(\gamma_5\Sigma(P)\not{b}). \quad (21)$$

These structure functions are found to depend upon various Lorentz scalars defined by

$$p^0 \equiv P^\mu u_\mu = \omega, \quad (22)$$

$$p^3 \equiv P^\mu b_\mu = -p_z, \quad (23)$$

$$p_\perp \equiv [(P^\mu u_\mu)^2 - (P^\mu b_\mu)^2 - (P^\mu P_\mu)^2]^{1/2}, \quad (24)$$

where $\omega, p_\perp, p_z$ are termed as Lorentz invariant energy, transverse momentum and longitudinal momentum respectively. The detailed calculation of all these structure functions is shown in the Appendix and results are quoted here:

$$\mathcal{A}(p_0,|\mathbf{p}|)=\frac{m_{th}^2}{|\mathbf{p}|^2}Q_1\left(\frac{p_0}{|\mathbf{p}|}\right), \tag{25}$$

$$\mathcal{B}(p_0,|\mathbf{p}|)=-\frac{m_{th}^2}{|\mathbf{p}|}\left[\frac{p_0}{|\mathbf{p}|}Q_1\left(\frac{p_0}{|\mathbf{p}|}\right)-Q_0\left(\frac{p_0}{|\mathbf{p}|}\right)\right], \tag{26}$$

$$\mathcal{C}(p_0,|\mathbf{p}|)=-4g^2C_FM^2\frac{p_z}{|\mathbf{p}|^2}Q_1\left(\frac{p_0}{|\mathbf{p}|}\right), \tag{27}$$

$$\mathcal{D}(p_0,|\mathbf{p}|)=-4g^2C_FM^2\frac{1}{|\mathbf{p}|}Q_0\left(\frac{p_0}{|\mathbf{p}|}\right), \tag{28}$$

where Q_0 and Q_1 are Legendre functions of the first and second kind, respectively, read as

$$Q_0(x)=\frac{1}{2}\ln\left(\frac{x+1}{x-1}\right), \tag{29}$$

$$Q_1(x)=\frac{x}{2}\ln\left(\frac{x+1}{x-1}\right)-1=xQ_0(x)-1, \tag{30}$$

with magnetic mass obtained as [74]

$$M^2(T,\mu,m_{f0},q_fB)=\frac{|q_fB|}{16\pi^2}\left(\frac{\pi T}{2m_{f0}}-\ln 2+\frac{7\mu^2\zeta(3)}{8\pi^2T^2}\right), \tag{31}$$

where ζ is the Riemann zeta function. The general covariant structure of quark self-energy Eq. (17) can be recast in terms of left-handed $[P_L=(\mathbb{I}-\gamma_5)/2]$ and right-handed $[P_R=(\mathbb{I}+\gamma_5)/2]$ chiral projection operators as

$$\Sigma(P)=-P_R\slashed{A}'P_L-P_L\slashed{B}'P_R, \tag{32}$$

with $\slashed{A}'$ and $\slashed{B}'$ defined as

$$\slashed{A}'=\mathcal{A}\slashed{P}+(\mathcal{B}+\mathcal{C})\slashed{u}+\mathcal{D}\slashed{b}, \tag{33}$$

$$\slashed{B}'=\mathcal{A}\slashed{P}+(\mathcal{B}-\mathcal{C})\slashed{u}-\mathcal{D}\slashed{b}. \tag{34}$$

Using Eqs. (9) and (32), the inverse fermion propagator can be written as

$$S^{*-1}(P)=\slashed{P}+P_R[\mathcal{A}\slashed{P}+(\mathcal{B}+\mathcal{C})\slashed{u}+\mathcal{D}\slashed{b}]P_L+P_L[\mathcal{A}\slashed{P}+(\mathcal{B}-\mathcal{C})\slashed{u}-\mathcal{D}\slashed{b}]P_R, \tag{35}$$

and using $P_{L,R}\gamma^\mu=\gamma^\mu P_{R,L}$ and $P_L\slashed{P}P_L=P_R\slashed{P}P_R=P_LP_R\slashed{P}=0$, we obtain

$$S^{*-1}(P)=P_R\slashed{L}P_L+P_L\slashed{R}P_R, \tag{36}$$

where $\slashed{L}$ and $\slashed{R}$ are

$$\slashed{L}=(1+\mathcal{A})\slashed{P}+(\mathcal{B}+\mathcal{C})\slashed{u}+\mathcal{D}\slashed{b}, \tag{37}$$

$$\slashed{R}=(1+\mathcal{A})\slashed{P}+(\mathcal{B}-\mathcal{C})\slashed{u}-\mathcal{D}\slashed{b}. \tag{38}$$

Thus, we get the effective quark propagator as

$$S^*(P)=\frac{1}{2}\left[P_L\frac{\slashed{L}}{L^2/2}P_R+P_R\frac{\slashed{R}}{R^2/2}P_L\right], \tag{39}$$

where

$$L^2=(1+\mathcal{A})^2P^2+2(1+\mathcal{A})(\mathcal{B}+\mathcal{C})p_0-2\mathcal{D}(1+\mathcal{A})p_z+(\mathcal{B}+\mathcal{C})^2-\mathcal{D}^2, \tag{40}$$

$$R^2=(1+\mathcal{A})^2P^2+2(1+\mathcal{A})(\mathcal{B}-\mathcal{C})p_0+2\mathcal{D}(1+\mathcal{A})p_z+(\mathcal{B}-\mathcal{C})^2-\mathcal{D}^2. \tag{41}$$

Next, we take the static limit $(p_0=0,|\mathbf{p}|\to 0)$ of $L^2/2$ and $R^2/2$, after expanding the Legendre functions involved in structure functions in power series of $\frac{|\mathbf{p}|}{p_0}$. Considering up to $\mathcal{O}(g^2)$, we obtain

$$\left.\frac{L^2}{2}\right|_{p_0=0,|\mathbf{p}|\to 0}=m_{th}^2+4g^2C_FM^2, \tag{42}$$

$$\left.\frac{R^2}{2}\right|_{p_0=0,|\mathbf{p}|\to 0}=m_{th}^2-4g^2C_FM^2. \tag{43}$$

The degenerate left- and right-handed modes get separated out in the presence of weak magnetic field and hence the thermal mass (squared) at finite chemical potential in the presence of weak magnetic field obtained as

$$m_L^2=m_{th}^2+4g^2C_FM^2, \tag{44}$$

$$m_R^2=m_{th}^2-4g^2C_FM^2, \tag{45}$$

which is opposite to the case of strong magnetic field where left- and right-handed chiral modes have the same mass [62]. The quasiparticle mass obtained above consists of pure thermal and magnetic contributions. The thermal mass is independent of chiral modes whereas the magnetic contribution depends on the chiral modes. The dispersion relation for both chiral modes of quarks at low and high momentum limit in the lowest Landau level is given by [66]

$$\omega_{L/R}(p_z) = m_{L/R} + \frac{p_z}{3}; \quad (p_z \ll m_{L/R}) \tag{46}$$

$$\omega_{L/R}(p_z) = |p_z| + \frac{m^2_{L/R}}{p_z}; \quad (p_z \gg m_{L/R}). \tag{47}$$

The form of dispersion relations in both low and high momentum limits even in the presence of magnetic field is similar to that in the absence of magnetic field and the masses in both limits are of the same order. However, the quasiparticle mass used in our computation is obtained from the static limit of the pole of the full quark propagator (up to one-loop quark self-energy), which is independent of low momentum and high momentum limits. Now, we will evaluate the charge and thermal transport coefficients in the presence of weak magnetic field at finite chemical potential for left- and right-handed modes separately as the system will not be in both modes simultaneously.

III. CHARGE TRANSPORT COEFFICIENTS

The Boltzmann transport equation governs the evolution of phase space density $f(x,p)$ associated with the partons in our system. The QGP is a relativistic plasma, since $T \gg$ any mass scale in the system. This validates the use of the relativistic Boltzmann transport equation (RBTE) to carry out our investigation. The RBTE for relativistic particle with a charge q in the presence of external electromagnetic field can be written as [75]

$$p^\mu \partial_\mu f(x,p) + qF^{\mu\nu} p_\nu \frac{\partial f(x,p)}{\partial p^\mu} = C[f], \tag{48}$$

where f is the distribution function deviated slightly from equilibrium distribution function (f_0) with $f = f_0 + \delta f$ ($\delta f \ll f_0$). $F^{\mu\nu}$ is the antisymmetric electromagnetic field tensor, $C[f]$ is the collision integral that describes the rate of change of distribution function by virtue of collisions. The general form of collision integral consists of absorption and emission terms in phase space volume element. This leads to nonlinear integro-differential equation which is very complicated to solve. Hence, we simplify the equation using relaxation-time approximation (RTA). Under relaxation time approximation, the external perturbation takes the system slightly away from equilibrium from which it relaxes towards the equilibrium exponentially with time scale τ. The collision integral under RTA takes the form as

$$C[f] \simeq -\frac{p^\mu u_\mu}{\tau}(f - f_0) \equiv -\frac{p^\mu u_\mu}{\tau}\delta f, \tag{49}$$

where u_μ is the fluid 4-velocity, τ is the thermal averaged relaxation time. Equation (48) in 3-notation can be written as

$$\frac{\partial f}{\partial t} + \mathbf{v}.\frac{\partial f}{\partial \mathbf{r}} + q(\mathbf{E} + \mathbf{v} \times \mathbf{B}).\frac{\partial f}{\partial \mathbf{p}} = -\frac{1}{\tau}(f - f_0). \tag{50}$$

We consider the spatially uniform $\frac{\partial f}{\partial \mathbf{r}} \approx 0$ and static medium $\frac{\partial f}{\partial t} = 0$ such that there are no space-time gradient. Then Eq. (50) simplifies to

$$q(\mathbf{E} + \mathbf{v} \times \mathbf{B}).\frac{\partial f}{\partial \mathbf{p}} = -\frac{1}{\tau}(f - f_0). \tag{51}$$

For the sake of simplicity of calculation, we choose the transverse electric and magnetic field as $\mathbf{E} = E\hat{x}$ and $\mathbf{B} = B\hat{z}$. This yields

$$f - qB\tau\left(v_x \frac{\partial f}{\partial p_y} - v_y \frac{\partial f}{\partial p_x}\right) = f_0 - qE\tau \frac{\partial f_0}{\partial p_x}. \tag{52}$$

In order to solve Eq. (52), we take the following *ansatz* of distribution function $f(p)$ as [76]

$$f(p) = f_0 - \tau q \mathbf{E}.\frac{\partial f_0}{\partial \mathbf{p}} - \boldsymbol{\xi}.\frac{\partial f_0}{\partial \mathbf{p}}, \tag{53}$$

and f_0 is given by

$$f_0(\mathbf{p}) = \frac{1}{e^{(\sqrt{\mathbf{p}^2 + m^2} - \mu)/T} + 1}, \tag{54}$$

which is the space and time independent solution to the Boltzmann equation and f_0 satisfies

$$\frac{\partial f_0}{\partial \mathbf{p}} = \mathbf{v}\frac{\partial f_0}{\partial \varepsilon}, \qquad \frac{\partial f_0}{\partial \varepsilon} = -\beta f_0(1 - f_0), \tag{55}$$

where $\varepsilon = \sqrt{\mathbf{p}^2 + m^2}$ is the single particle energy. Using the *ansatz* Eq. (53) in Eq. (52), we get

$$\left(f_0 - \tau q \mathbf{E}.\frac{\partial f_0}{\partial \mathbf{p}} - \boldsymbol{\xi}.\frac{\partial f_0}{\partial \mathbf{p}}\right) - qB\tau\left(v_x \frac{\partial}{\partial p_y} - v_y \frac{\partial}{\partial p_x}\right)$$
$$\left(f_0 - \tau q \mathbf{E}.\frac{\partial f_0}{\partial \mathbf{p}} - \boldsymbol{\xi}.\frac{\partial f_0}{\partial \mathbf{p}}\right) = f_0 - qE\tau \frac{\partial f_0}{\partial p_x}. \tag{56}$$

The first term in the parentheses on the left-hand side of Eq. (56) can be rewritten as

$$\left(f_0 - \tau q\mathbf{E}.\frac{\partial f_0}{\partial \mathbf{p}} - \boldsymbol{\xi}.\frac{\partial f_0}{\partial \mathbf{p}}\right) = f_0 + \beta\tau qEv_x f_0 + (\boldsymbol{\xi}.\mathbf{v})\beta f_0. \tag{57}$$

Neglecting the f_0^2 terms at high temperature and using the following second order partial derivatives,

$$\frac{\partial^2 f_0}{\partial p_y p_x} = \frac{\beta p_x p_y f_0}{\varepsilon^2}\left(\beta + \frac{1}{\varepsilon}\right), \tag{58}$$

$$\frac{\partial^2 f_0}{\partial p_y p_z} = \frac{\beta p_y p_z f_0}{\varepsilon^2}\left(\beta + \frac{1}{\varepsilon}\right), \tag{59}$$

$$\frac{\partial^2 f_0}{\partial p_y^2} = -\beta\left[\frac{f_0}{\varepsilon} - \frac{f_0 p_y^2}{\varepsilon^2}\left(\beta + \frac{1}{\epsilon}\right)\right], \tag{60}$$

the second term on the left-hand side of Eq. (56) gets reduced to

$$qB\tau\left(v_x\frac{\partial}{\partial p_y} - v_y\frac{\partial}{\partial p_x}\right)\left(f_0 - \tau q\mathbf{E}.\frac{\partial f_0}{\partial \mathbf{p}} - \boldsymbol{\xi}.\frac{\partial f_0}{\partial \mathbf{p}}\right)$$
$$= qB\tau\beta\left(\frac{\xi_y v_x}{\varepsilon} - \frac{\xi_x v_y}{\varepsilon} - \frac{v_y \tau qE}{\varepsilon}\right)f_0. \tag{61}$$

Combining Eqs. (57) and (61), Eq. (56) is obtained as

$$\frac{\tau qBqEv_y}{\varepsilon} - \frac{qB}{\varepsilon}(v_x\xi_y - v_y\xi_x) + \frac{1}{\tau}\left(\xi_x\frac{p_x}{\varepsilon} + \xi_y\frac{p_y}{\varepsilon} + \xi_z\frac{p_z}{\varepsilon}\right) = 0. \tag{62}$$

The above equation should be satisfied for any value of velocity; therefore, comparing the coefficients of v_x, v_y and v_z of Eq. (62), we get

$$\xi_z = 0, \tag{63}$$

$$\omega_c\tau qE + \omega_c\xi_x + \frac{\xi_y}{\tau} = 0, \tag{64}$$

$$\frac{\xi_x}{\tau} - \omega_c\xi_y = 0, \tag{65}$$

where $\omega_c = \frac{qB}{\varepsilon}$ is termed as the cyclotron frequency. Solving for ξ_x and ξ_y, we have

$$\xi_x = \frac{-\omega_c^2\tau^3 qE}{(\omega_c^2\tau^2 + 1)}; \qquad \xi_y = \frac{-\omega_c\tau^2 qE}{(\omega_c^2\tau^2 + 1)}. \tag{66}$$

Using Eq. (80) in Eq. (53), the distribution function $f(p)$ for quarks simplifies to

$$f(p) = f_0 - \frac{qEv_x\tau}{(1+\omega_c^2\tau^2)}\left(\frac{\partial f_0}{\partial\varepsilon}\right) + \frac{qEv_y\omega_c\tau^2}{(1+\omega_c^2\tau^2)}\left(\frac{\partial f_0}{\partial\varepsilon}\right), \tag{67}$$

and for antiquarks $(f \to \bar{f}, q \to -q, \omega_c \to -\omega_c)$,

$$\bar{f}(p) = \overline{f_0} + \frac{qEv_x\tau}{(1+\omega_c^2\tau^2)}\left(\frac{\partial \bar{f}_0}{\partial\varepsilon}\right) + \frac{qEv_y\omega_c\tau^2}{(1+\omega_c^2\tau^2)}\left(\frac{\partial \bar{f}_0}{\partial\varepsilon}\right). \tag{68}$$

The induced current in the system as a result of external electromagnetic fields can be written as

$$j^i = \sigma_{\text{Ohmic}}\delta^{ij}E_j + \sigma_{\text{Hall}}\epsilon^{ij}E_j, \tag{69}$$

where σ_{Ohmic} and σ_{Hall} are Ohmic and Hall conductivities respectively, ϵ_{ij} is the 2×2 antisymmetric unity tensor, with $\epsilon_{12} = -\epsilon_{21} = 1$. It is clear from the above equation that σ_{Ohmic} describes the longitudinal response (current along the direction of electric field) and σ_{Hall} describes the transverse response (current transverse to the electric field). Further, the induced current can be written in terms of deviation δf $(\delta\bar{f})$ from f_0 $(\bar{f}_0)$ as

$$\mathbf{j} = g_f\int\frac{d^3p}{(2\pi)^3}\mathbf{v}(q\delta f(p) + \bar{q}\delta\bar{f}(p)), \tag{70}$$

where $\bar{q}$ is the charge of antiparticle and $g_f = 3\times 2$ is the color and spin degeneracy factor of fermions. Using Eqs. (69) and (70), the Ohmic and Hall conductivity for a system of multiple charge species can be written as

$$\sigma_{\text{Ohmic}} = \frac{1}{6\pi^2 T}\sum_f g_f q_f^2\tau_f\int dp\frac{p^4}{\varepsilon_f^2}\frac{1}{(1+\omega_c^2\tau_f^2)}[f_f^0(1-f_f^0) + \bar{f}_f^0(1-\bar{f}_f^0)], \tag{71}$$

$$\sigma_{\text{Hall}} = \frac{1}{6\pi^2 T}\sum_f g_f q_f^2\tau_f^2\int dp\frac{p^4}{\varepsilon_f^2}\frac{\omega_c}{(1+\omega_c^2\tau_f^2)}[f_f^0(1-f_f^0) - \bar{f}_f^0(1-\bar{f}_f^0)], \tag{72}$$

where f stands for flavor and here we have used $f = $ up (u), down (d). The relaxation time for quarks (antiquarks) used above for calculation of conductivities is given by [77], where massless u- and d-quarks were considered with $\mu \ll T$:

$$\tau_{q(\bar{q})} = \frac{1}{5.1T\alpha_s^2 \log(\frac{1}{\alpha_s})(1 + 0.12(2N_f + 1))}.$$

It was argued in [78] that finite parton mass has little effect on scattering cross section and hence on relaxation time. This leads to the qualitatively same result for massless and massive partons. The current light quark ($m_{u,d}$) masses are chosen to be 0.1 times the strange quark mass (m_{s0}) which is in compliance with chiral perturbation theory [79,80]. The parameters were adjusted to get the best fitted lattice data with $m_{s0} = 80$ MeV [81]. The Ohmic and Hall conductivity obtained above is defined by current which appears due to the effect of an electric and magnetic field when there is no temperature gradient or we can say isothermal Ohmic and Hall conductivity. As discussed in the quasiparticle model, we will incorporate the quasiparticle mass which was obtained to be different for left- and right-handed chiral modes. $u(\bar{u})$ and $d(\bar{d})$ quarks are spin-$\frac{1}{2}$ particles and they can assume right handedness or left handedness depending on their up or down spin with respect to their direction of motion. We have taken into account both modes for up and down quarks and computed the conductivities for L and R modes separately. In the case of baryonic symmetry i.e., at zero quark chemical potential, the distribution function for quarks and antiquarks becomes equal and hence Hall conductivity vanishes.

IV. HEAT TRANSPORT COEFFICIENTS

In the nonrelativistic case, the heat equation is obtained by the validity of the first and second laws of thermodynamics, where the flow of heat is proportional to the temperature gradient and the proportionality factor is called the thermal conductivity. We are intended to study the thermal conductivity in the system of partons. The heat flow 4-vector which is defined to be the difference between energy diffusion and enthalpy diffusion is given as [82]

$$Q_\mu = \Delta_{\mu\alpha} T^{\alpha\beta} u_\beta - h \Delta_{\mu\alpha} N^\alpha, \tag{73}$$

where $\Delta_{\mu\alpha} = g_{\mu\alpha} - u_\mu u_\alpha$ is the projection operator. N^α is characterized as first moment of distribution function which corresponds to the particle four-flow vector as

$$N^\alpha = \sum_f g_f \int \frac{d^3p}{(2\pi)^3} \frac{p^\alpha}{\varepsilon_f} [f_f - \bar{f}_f], \tag{74}$$

whereas, $T^{\alpha\beta}$ is characterized as second moment of distribution function which corresponds to the energy-momentum tensor as

$$T^{\alpha\beta} = \sum_f g_f \int \frac{d^3p}{(2\pi)^3} \frac{p^\alpha p^\beta}{\varepsilon_f} (f_f + \bar{f}_f) + g_g \int \frac{d^3p}{(2\pi)^3} \frac{p^\alpha p^\beta}{\varepsilon_g} f_g, \tag{75}$$

where, $f_f, \bar{f}_f$ and f_g are quark, antiquark and gluon distribution function, ε_g is the single particle energy for gluons and $g_g = 8 \times 2$ is the degeneracy factor of the gluons. We can obtain the particle number density, energy density and pressure from the above equation as $n = N^\alpha u_\alpha$, $e = u_\alpha T^{\alpha\beta} u_\beta$ and $P = -\Delta_{\alpha\beta} T^{\alpha\beta}/3$ respectively. Therefore, enthalpy per particle can be obtained as $h = (e + P)/n$. The heat flow 4-vector in the rest frame of the heat bath is orthogonal to fluid 4-velocity, i.e., $Q_\mu u^\mu = 0$. Thus, heat flow is spatial which can be written in terms of infinitesimal changes in the distribution function as

$$\mathbf{Q} = \sum_f g_f \int \frac{d^3p}{(2\pi)^3} \frac{\mathbf{p}}{\varepsilon_f} [(\varepsilon_f - h_f) \delta f_f + (\varepsilon_f + \bar{h}_f) \delta \bar{f}_f] + g_g \int \frac{d^3p}{(2\pi)^3} \mathbf{p} \delta f_g. \tag{76}$$

The particle four-flow and energy-momentum tensor can be decomposed with respect to an arbitrary normalized time-like four vector, $u^\mu = \gamma(1, \vec{v})$, where $u^\mu u_\mu = 1$. The most general decomposition is given as [83,84]

$$N^\mu = n u^\mu + v^\mu, \tag{77}$$

$$T^{\mu\nu} = -P g^{\mu\nu} + w u^\mu u^\nu + \pi^{\mu\nu}, \tag{78}$$

where v^μ is the particle diffusion current, $w = e + P$ is the heat function per unit volume, and $\pi^{\mu\nu}$ is the shear-stress tensor. Using the continuity equation and law of increase of entropy, the required form of symmetrical 4-tensor $\pi^{\mu\nu}$ and 4-vector v^μ were obtained to be as [83]

$$\pi^{\mu\nu} = -c\eta \left(\frac{\partial u^\mu}{\partial x_\nu} + \frac{\partial u^\nu}{\partial x_\mu} - u^\mu u_\alpha \frac{\partial u^\nu}{\partial x_\alpha} - u^\mu u^\alpha \frac{\partial u^\mu}{\partial x^\alpha} \right) - \left(\zeta - \frac{2}{3}\eta \right) \frac{\partial u^\alpha}{\partial x^\alpha} (g^{\mu\nu} - u^\mu u^\nu), \tag{79}$$

$$v^\mu = \frac{\kappa}{c} \left(\frac{nT}{w} \right)^2 \left[\frac{\partial}{\partial x_\mu} \left(\frac{\mu}{T} \right) - u^\mu u^\alpha \frac{\partial}{\partial x^\alpha} \left(\frac{\mu}{T} \right) \right]. \tag{80}$$

Here, η and ζ are shear and bulk viscosity coefficients and κ is the thermal conductivity, taken in accordance with their nonrelativistic definitions. The zero particle flux ($nu^i + v^i = 0$) corresponds to the pure thermal conduction. The spatial components $u^i = -v^i/n$ of the 4-velocity are of the first order in the gradients; since $\pi^{\mu\nu}$, v^μ are written only as far as this order, the 4-velocity component u^0 must be taken as unity. To the same accuracy, omitting the second term in the square bracket of Eq. (80), the energy flux density from $T^{\mu\nu}$ is given as

$$cT^{0i} = cwu^0u^i = -cwv^i/n = -\kappa\frac{nT^2}{e+P}\left[\frac{\partial}{\partial x_i}\left(\frac{\mu}{T}\right)\right], \tag{81}$$

which relates the energy flux density/heat flow with the gradient of thermodynamical potential ($U = \mu/T$) as in Navier-Stokes theory. In terms of 4-gradient, the above equation can be written as

$$Q_\mu = -\kappa\frac{nT^2}{e+P}\nabla_\mu U, \tag{82}$$

where κ is the thermal conductivity and ∇_μ is the 4-gradient, $\nabla_\mu = \partial_\mu - u_\mu u_\nu \partial^\nu$. The entropy density $[s = s(e,n)]$ in equilibrium state in terms of energy density, pressure and chemical potential can be written as [85]

$$s = \left(\frac{e+P}{T}\right) - \left(\frac{\mu}{T}\right)n. \tag{83}$$

Further, the inverse of temperature (T^{-1}) and thermodynamic potential (U) can be defined as the partial derivative of $s(e,n)$:

$$\mathrm{d}s = \frac{1}{T}\mathrm{d}e - U\mathrm{d}n. \tag{84}$$

Using Eqs. (83) and (84), we obtain

$$\mathrm{d}\left(\frac{P}{T}\right) = -e\mathrm{d}\left(\frac{1}{T}\right) + n\mathrm{d}U, \qquad \frac{\mathrm{d}P}{nT} = \mathrm{d}U + \frac{1}{T^2}\left(\frac{P+e}{n}\right)\mathrm{d}T. \tag{85}$$

Generalizing it to the 4-gradient, the heat flow can be rewritten as

$$Q_\mu = \kappa\left[\nabla_\mu T - \frac{T}{e+P}\nabla_\mu P\right], \tag{86}$$

and in the local rest frame, the spatial component of heat flow can be written as

$$\mathbf{Q} = -\kappa\left[\frac{\partial T}{\partial \mathbf{x}} - \frac{T}{nh}\frac{\partial P}{\partial \mathbf{x}}\right]. \tag{87}$$

One can thus obtain the thermal conductivity (κ) by comparing Eqs. (76) and (87). We will first calculate the contribution of quarks and antiquarks to the thermal conductivity. So now, expressing the relativistic Boltzmann transport equation in terms of gradients of flow velocity and temperature in relaxation time approximation as

$$p^\mu\partial_\mu T\left(\frac{\partial f}{\partial T}\right) + p^\mu\partial_\mu(p^\nu u_\nu)\left(\frac{\partial f}{\partial p^0}\right) + q\left(F^{0j}p_j\frac{\partial f}{\partial p^0} + F^{j0}p_0\frac{\partial f}{\partial p^j} + F^{ij}p_j\frac{\partial f}{\partial p^i} + F^{ji}p_i\frac{\partial f}{\partial p^j}\right) = -\frac{p^\mu u_\mu}{\tau}\delta f, \tag{88}$$

where $p_0 = \varepsilon - \mu$ and for very small μ, it can be approximated as $p_0 \approx \varepsilon$. Using the following partial derivatives,

$$\frac{\partial f_0}{\partial T} = \frac{\varepsilon}{T^2}f_0(1-f_0), \tag{89}$$

$$\frac{\partial f_0}{\partial p^0} = -\frac{1}{T}f_0(1-f_0), \tag{90}$$

$$\frac{\partial f_0}{\partial p_j} = -\frac{p_j}{Tp_0}f_0(1-f_0), \tag{91}$$

Eq. (88) is given as

$$\begin{aligned} -\frac{\delta f}{\tau} &= \frac{f_0(1-f_0)}{p^0}\left[p^\mu\partial_\mu T\left(\frac{p^0}{T^2}\right) - \frac{p^\mu\partial_\mu(p^\nu u_\nu)}{T} - \frac{q}{T}(F^{0j}p_j + F^{j0}p_j)\right] + \frac{q}{p^0}\left(F^{ij}p_j\frac{\partial f}{\partial p^i} + F^{ji}p_i\frac{\partial f}{\partial p^j}\right) \\ &= \frac{1}{T}f_0(1-f_0)\left[\frac{1}{T}(p^0\partial_0 T + p^j\partial_j T) + T\partial_0\left(\frac{\mu}{T}\right) + \frac{p^jT}{p^0}\partial_j\left(\frac{\mu}{T}\right) - \frac{1}{p^0}(p^0p^\nu\partial_0u_\nu + p^jp^\nu\partial_ju_\nu) \right. \\ &\quad \left. - 2q\frac{\mathbf{E}.\mathbf{p}}{p^0}\right] + q(\mathbf{v}\times\mathbf{B}).\frac{\partial f}{\partial \mathbf{p}}, \end{aligned} \tag{92}$$

where $2F_{ij} = \epsilon_{ijk}B^k$. Now, exerting the energy-momentum conservation $(\partial_0 u_\mu = \frac{\nabla_\mu P}{nh})$ along with relativistic Gibbs-Duhem relation,

$$\partial_j\left(\frac{\mu}{T}\right) = \frac{-h}{T^2}\left(\partial_j T - \frac{T}{nh}\partial_j P\right),$$

we obtain Eq. (92) as

$$-\frac{\delta f}{\tau} = \frac{1}{T}f_0(1-f_0)\left[\frac{1}{T}(p^0\partial_0 T) + \left(\frac{p^0-h}{p^0}\right)\frac{p^j}{T}\left(\partial_j T - \frac{T}{nh}\partial_j P\right) + T\partial_0\left(\frac{\mu}{T}\right) - p^j p^\nu(\partial_j u_\nu) - 2q\frac{\mathbf{E}.\mathbf{p}}{p^0}\right] + q(\mathbf{v}\times\mathbf{B}).\frac{\partial f}{\partial \mathbf{p}}, \tag{93}$$

where $\frac{\partial f}{\partial \mathbf{p}} = \frac{\partial}{\partial \mathbf{p}}(f_0 + \delta f)$ and $\frac{\partial f_0}{\partial p^j} \propto v^j$, therefore the Lorentz term vanishes for the equilibrium distribution function and we get

$$-\frac{\delta f}{\tau} = \frac{1}{T}f_0(1-f_0)\left[\frac{p_0}{T}\partial_0 T + \left(\frac{p^0-h}{p^0}\right)\frac{p^j}{T}\left(\partial_j T - \frac{T}{nh}\partial_j P\right) + T\partial_0\left(\frac{\mu}{T}\right) - \frac{p^j p^\nu}{p_0}(\partial_j u_\nu) - \frac{2q}{p_0}(\mathbf{E}.\mathbf{p})\right] + q(\mathbf{v}\times\mathbf{B})\frac{\partial(\delta f)}{\partial \mathbf{p}}. \tag{94}$$

Now, choosing the *ansatz* for infinitesimal deviation (δf) from f_0 as [57]

$$\delta f = (\mathbf{p}.\chi)\frac{\partial f_0}{\partial \varepsilon}, \tag{95}$$

where χ in turn is related to thermal driving force and magnetic field in medium and takes the form as

$$\chi = a_1\mathbf{c} + a_2\mathbf{Y} + a_3(\mathbf{Y}\times\mathbf{c}). \tag{96}$$

Here, $\mathbf{c} = \frac{\mathbf{B}}{|\mathbf{B}|}$ and $\mathbf{Y} = \frac{\nabla T}{T} - \frac{\nabla P}{nh}$. Using Eqs. (95) and (94), we have

$$\frac{\mathbf{p}.\chi}{\tau} = \left[\frac{p_0}{T}\partial_0 T + \left(\frac{p^0-h}{p^0}\right)\frac{\mathbf{p}}{T}.\left(\nabla T - \frac{T}{nh}\nabla P\right) + T\partial_0\left(\frac{\mu}{T}\right) - \frac{p^j p^\nu}{p_0}(\partial_j u_\nu) - \frac{2q}{p_0}(\mathbf{E}.\mathbf{p}) - q(\mathbf{v}\times\mathbf{B}).\chi\right]. \tag{97}$$

The derivative is split up covariantly into time and space parts: $\partial_\mu = u_\mu D + \nabla_\mu$, where $D = u^\mu\partial_\mu = (\partial_t, 0)$ and $\nabla_\mu = \partial_\mu - u_\mu D = (0, \partial_i)$. The time derivative term $[\partial_0 T, \partial_0(\frac{\mu}{T})]$ can be written in terms of $\nabla_\mu u^\mu$ by using the following relations [77,82]:

$$\frac{DT}{T} = -\left(\frac{\partial P}{\partial e}\right)_n \nabla_\mu u^\mu, \tag{98}$$

$$TD\left(\frac{\mu}{T}\right) = -\left(\frac{\partial P}{\partial n}\right)_e \nabla_\mu u^\mu. \tag{99}$$

Therefore, Eq. (97) becomes

$$\frac{\mathbf{p}.\chi}{\tau} = \left[-p_0\left(\frac{\partial P}{\partial e}\right)_n \nabla_\mu u^\mu + \left(\frac{p^0-h}{p^0}\right)\frac{\mathbf{p}}{T}.\left(\nabla T - \frac{T}{nh}\nabla P\right) - \left(\frac{\partial P}{\partial n}\right)_e \nabla_\mu u^\mu - \frac{p^j p^\nu}{p_0}(\partial_j u_\nu) - \frac{2q}{p_0}(\mathbf{E}.\mathbf{p}) - q(\mathbf{v}\times\mathbf{B}).\chi\right]. \tag{100}$$

$$\frac{p^0}{\tau}\mathbf{v}.(a_1\mathbf{c} + a_2\mathbf{Y} + a_3(\mathbf{Y}\times\mathbf{c})) = (p^0-h)\mathbf{v}.\mathbf{Y} - q(\mathbf{v}\times\mathbf{B}).a_2\mathbf{Y} - q(\mathbf{v}\times\mathbf{B}).a_3(\mathbf{Y}\times\mathbf{c}), \tag{101}$$

where $(\mathbf{v}\times\mathbf{B}).\mathbf{c} = 0$. Using the properties of scalar triple product, the parameters a_1, a_2 and a_3 can be obtained by comparing the terms with different tensor structures in both sides of Eq. (101) independently, and we have

$$\frac{\varepsilon}{\tau}a_1 = a_3 q|\mathbf{B}|(\mathbf{c}.\mathbf{Y}), \tag{102}$$

$$\frac{\varepsilon}{\tau}a_2 = (\varepsilon - h) - a_3 q|\mathbf{B}|, \tag{103}$$

$$\frac{\varepsilon}{\tau}a_3 = a_2 q|\mathbf{B}|, \tag{104}$$

where $p^0 \approx \varepsilon$, $|\mathbf{B}| = B$. Employing the above equations and defining $\omega_c = \frac{qB}{\varepsilon}$, the parameters reduced to the following forms:

$$a_1 = \frac{\tau^3}{\varepsilon}\frac{(\varepsilon-h)}{(1+\omega_c^2\tau^2)}\omega_c^2(\mathbf{c}.\mathbf{Y}),$$
$$a_2 = \frac{\tau}{\varepsilon}\frac{(\varepsilon-h)}{(1+\omega_c^2\tau^2)},$$
$$a_3 = \frac{\tau^2}{\varepsilon}\frac{(\varepsilon-h)}{(1+\omega_c^2\tau^2)}\omega_c. \tag{105}$$

Substituting a_1, a_2, a_3 in Eq. (96), we obtain the δf correction to the distribution function in the presence of the weak magnetic field from Eq. (95) as

$$\delta f = \frac{\tau(\varepsilon - h)}{(1+\omega_c^2\tau^2)}[\mathbf{v}.\mathbf{Y} + \tau\omega_c\mathbf{v}.(\mathbf{Y}\times\mathbf{c}) + \tau^2\omega_c^2(\mathbf{c}.\mathbf{Y})(\mathbf{v}.\mathbf{c})]\frac{\partial f_0}{\partial\varepsilon}. \tag{106}$$

Similarly, $\delta\bar{f}$ can be calculated as

$$\delta\bar{f} = \frac{\tau(\varepsilon+\bar{h})}{(1+\omega_c^2\tau^2)}[\mathbf{v}.\mathbf{Y} - \tau\omega_c\mathbf{v}.(\mathbf{Y}\times\mathbf{c}) + \tau^2\omega_c^2(\mathbf{c}.\mathbf{Y})(\mathbf{v}.\mathbf{c})]\frac{\partial\bar{f}_0}{\partial\varepsilon}, \tag{107}$$

where $\bar{h}$ is the enthalpy per particle for antiquarks. Using Eqs. (106) and (107) in (76), the heat flow in the weakly magnetized medium, generalizing to the system of different charged particles takes the form as

$$\mathbf{Q} = \sum_f g_f\tau_f\int\frac{d^3p}{(2\pi)^3}\frac{\mathbf{p}}{\varepsilon_f}\left[\frac{(\varepsilon_f - h_f)^2}{(1+\omega_c^2\tau_f^2)}(\mathbf{v}.\mathbf{Y} + \tau_f\omega_c\mathbf{v}.(\mathbf{Y}\times\mathbf{c}) + \tau_f^2\omega_c^2(\mathbf{c}.\mathbf{Y})(\mathbf{v}.\mathbf{c}))\frac{\partial f_f^0}{\partial\varepsilon_f} + \frac{(\varepsilon_f+\bar{h}_f)^2}{(1+\omega_c^2\tau_f^2)}(\mathbf{v}.\mathbf{Y} - \tau_f\omega_c\mathbf{v}.(\mathbf{Y}\times\mathbf{c}) + \tau_f^2\omega_c^2(\mathbf{c}.\mathbf{Y})(\mathbf{v}.\mathbf{c}))\frac{\partial\bar{f}_f^0}{\partial\epsilon_f}\right], \tag{108}$$

where h_f and $\bar{h}_f$ is the enthalpy per particle of quarks and antiquarks for fth flavor respectively. We will simplify the calculation by fixing the direction of $\mathbf{B}$ along the z-axis and temperature gradient in the x-y plane.

$$\mathbf{Q} = -\kappa_0 T\mathbf{Y} - \kappa_1 T(\mathbf{Y}\times\mathbf{c}), \tag{109}$$

where thermal transport coefficients in weakly magnetized medium, $\kappa_0(=\kappa_q+\kappa_g)$ and κ_1, can be defined as

$$\kappa_0 = \sum_f\frac{g_f\tau_f}{6\pi^2T^2}\int dp\frac{p^4}{\varepsilon_f^2}\left[\frac{(\varepsilon_f-h_f)^2}{(1+\omega_c^2\tau_f^2)}f_f^0(1-f_f^0) + \frac{(\varepsilon_f+\bar{h}_f)^2}{(1+\omega_c^2\tau_f^2)}\bar{f}_f^0(1-\bar{f}_f^0)\right] + \kappa_g, \tag{110}$$

and

$$\kappa_1 = \sum_f\frac{g_f\tau_f^2}{6\pi^2T^2}\int dp\frac{p^4}{\varepsilon_f^2}\left[\frac{(\varepsilon_f-h_f)^2\omega_c}{(1+\omega_c^2\tau_f^2)}f_f^0(1-f_f^0) - \frac{(\varepsilon_f+\bar{h}_f)^2\omega_c}{(1+\omega_c^2\tau_f^2)}\bar{f}_f^0(1-\bar{f}_f^0)\right], \tag{111}$$

where f stands for fth flavor. Similar to the discussion of charge transport coefficients, here we have thermal (κ_0) and Hall-type thermal conductivity (κ_1). Hall-type thermal conductivity emerges due to the transverse temperature gradient which is induced by the action of the magnetic field perpendicular to the initial direction of heat current and would be contributed by quarks and antiquarks. So far, we have obtained the contribution due to quarks and antiquarks to the thermal conductivity. Now, we will calculate the gluonic contribution to thermal conductivity.

Since gluons do not interact with the electromagnetic field therefore Eq. (88) for gluons assumes the form as

$$p^\mu\partial_\mu T\left(\frac{\partial f_g}{\partial T}\right) + p^\mu\partial_\mu(p^\nu u_\nu)\left(\frac{\partial f_g}{\partial p_g^0}\right) = -\frac{p^\mu u_\mu}{\tau}\delta f_g, \tag{112}$$

where $f_g = 1/(e^{\varepsilon_g/T}-1)$, $p_g^0 = \varepsilon_g$ is the single particle energy of gluon. Using the following partial derivative,

$$\frac{\partial f_g}{\partial T} = \frac{\varepsilon}{T^2}f_g(1+f_g), \tag{113}$$

$$\frac{\partial f_g}{\partial p_g^0} = -\frac{1}{T}f_g(1+f_g), \tag{114}$$

Eq. (112) can be rewritten as

$$\frac{1}{T}f_g(1+f_g)\left[\frac{1}{T}(p_g^0DT + p^j\nabla_jT) + TD\left(\frac{\mu}{T}\right) + \frac{p^jT}{p_g^0}\nabla_j\left(\frac{\mu}{T}\right) - \frac{1}{p_g^0}(p_g^0p^\nu\partial_0u_\nu + p^jp^\nu\partial_ju_\nu)\right] = -\frac{\delta f_g}{\tau_g}. \tag{115}$$

Considering only thermal driving forces and taking the gluon chemical potential to be zero, we obtain the equation as

$$\frac{1}{T}f_g(1+f_g)\left[p^j\left(\frac{\nabla_jT}{T} - \frac{\nabla_jP}{nh}\right)\right] = -\frac{\delta f_g}{\tau_g}, \tag{116}$$

where τ_g is thermal relaxation time for gluons given as [77]

$$\tau_g = \frac{1}{22.5T\alpha_s^2\log(\frac{1}{\alpha_s})(1+0.06N_f)}. \tag{117}$$

Putting δf_g in Eq. (76) and comparing with Eq. (82), we obtain the gluonic contribution to the thermal conductivity as

$$\kappa_g = \frac{g_g \tau_g}{6\pi^2 T^2} \int dp\, p^4 f_g (1 + f_g). \tag{118}$$

Therefore, thermal conductivity due to quarks, antiquarks and gluons along the initial direction of heat current is given by

$$\kappa_0 = \sum_f \frac{g_f \tau_f}{6\pi^2 T^2} \int dp \frac{p^4}{\varepsilon_f^2} \left(\frac{(\varepsilon_f - h_f)^2}{(1+\omega_c^2 \tau_f^2)} f_f^0 (1 - f_f^0) + \frac{(\varepsilon_f + \bar{h}_f)^2}{(1+\omega_c^2 \tau_f^2)} \bar{f}_f^0 (1 - \bar{f}_f^0) \right) + \frac{g_g \tau_g}{6\pi^2 T^2} \int dp\, p^4 f_g (1 + f_g). \tag{119}$$

Gluons will not contribute to κ_1 because the Lorentz force will not change their direction of motion. The thermal conductivity is obtained from heat current in temperature gradient on the condition that there is no electric current [86]. Hall-type thermal conductivity is the thermal analog of classical Hall effect where temperature plays the role of voltage and heat flow replaces the electric current [87] and it is the Lorentz force acting on charged particles affecting the curvature of the carrier's trajectories through the magnetic field. At zero chemical potential, κ_1 will not vanish due to the unequal contribution from quarks and antiquarks in the same direction, unlike in the case of Hall conductivity in charge transport.

V. RESULTS AND DISCUSSIONS

In this section, we will discuss the results regarding the Ohmic and Hall conductivity, thermal and Hall-type thermal conductivity and further Knudsen number and Wiedemann-Franz law as their application.

A. Ohmic and Hall conductivity

In Fig. 2, we have shown the variation of ratio of Ohmic conductivity to temperature ($\sigma_{\rm Ohmic}/T$) with respect to temperature for zero and finite magnetic field at nonzero chemical potential ($\mu = 30$ MeV). It is evident that the magnitude of $\sigma_{\rm Ohmic}/T$ gets a decrease in the presence of magnetic field as shown in Figs. 2(a) and 2(b). The difference between the magnitude of conductivities for L and R modes increases with an increase in magnetic field due to different effective quark mass for L and R modes, Eq. (44). This can also be deduced from the plots of distribution function of quark for left-handed and right-handed mode at fixed momentum and temperature shown in Figs. 3 and 4 respectively, where $T_c \simeq 160$ MeV is the deconfinement temperature from hadron phase to QGP phase. Further, $\sigma_{\rm Ohmic}/T$ for L mode decreases with magnetic field whereas it shows increasing trend for R mode. This behavior of $\sigma_{\rm Ohmic}/T$ with magnetic field for L and R modes is attributed to the factor $\frac{\tau}{\varepsilon^2(1+\omega_c^2\tau^2)}$. The thermal mass squared with magnetic field correction for the left(right)-handed mode is $m_{L(R)}^2 = m_{th}^2 \pm 4g^2 C_F M^2$, which is found to increase (decrease) with magnetic field. The appearance of this mass in the denominator of $\frac{\tau}{\varepsilon^2(1+\omega_c^2\tau^2)}$ factor leads to the decreasing (increasing) behavior of $\sigma_{\rm Ohmic}/T$ for left (right)-handed mode. The increasing behavior of $\sigma_{\rm Ohmic}/T$ with temperature for both modes could be due to the Boltzmann factor $\exp(-\varepsilon(p)/T)$ in the distribution function. Figure 5 shows the variation of normalized Ohmic conductivity at different constant values of quark chemical potential for eB $= 0.1 m_\pi^2$, where it increases with increase in quark chemical potential for both modes. With increasing quark chemical potential the

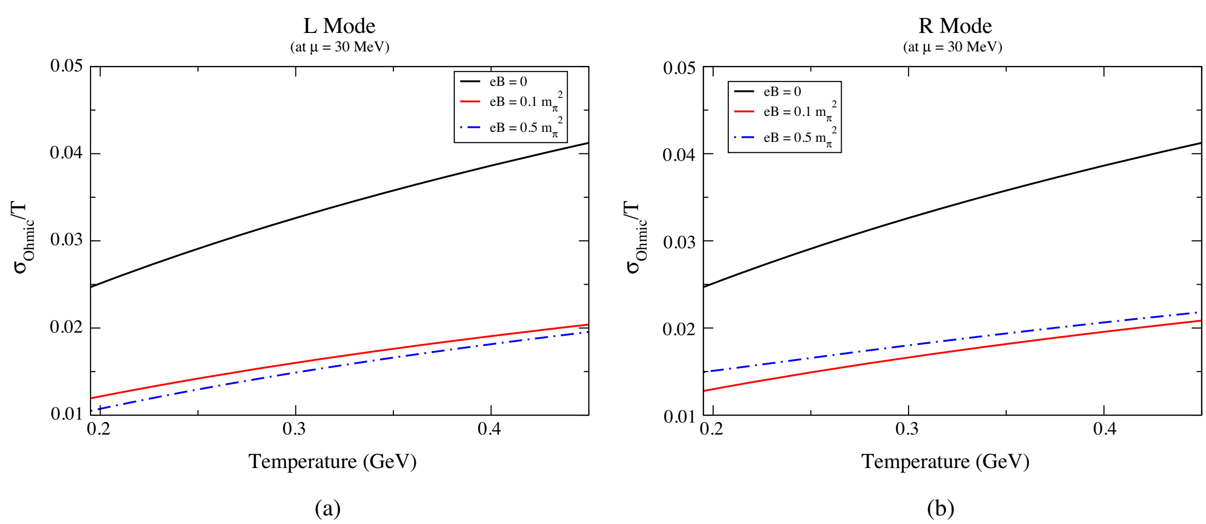

FIG. 2. Variation of $\sigma_{\rm Ohmic}/T$ for L mode (a) and R mode (b) with temperature at different fixed values of magnetic field.

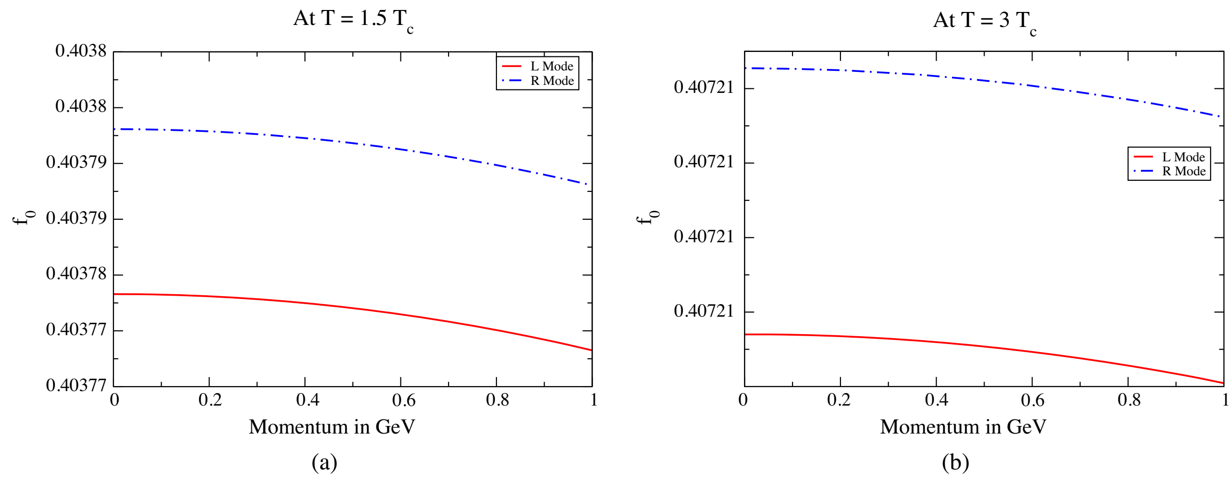

FIG. 3. Variation of distribution function of quark (f_0) in left- and right-handed mode with temperature at low (a) and high momentum (b), where effective quark mass has been used.

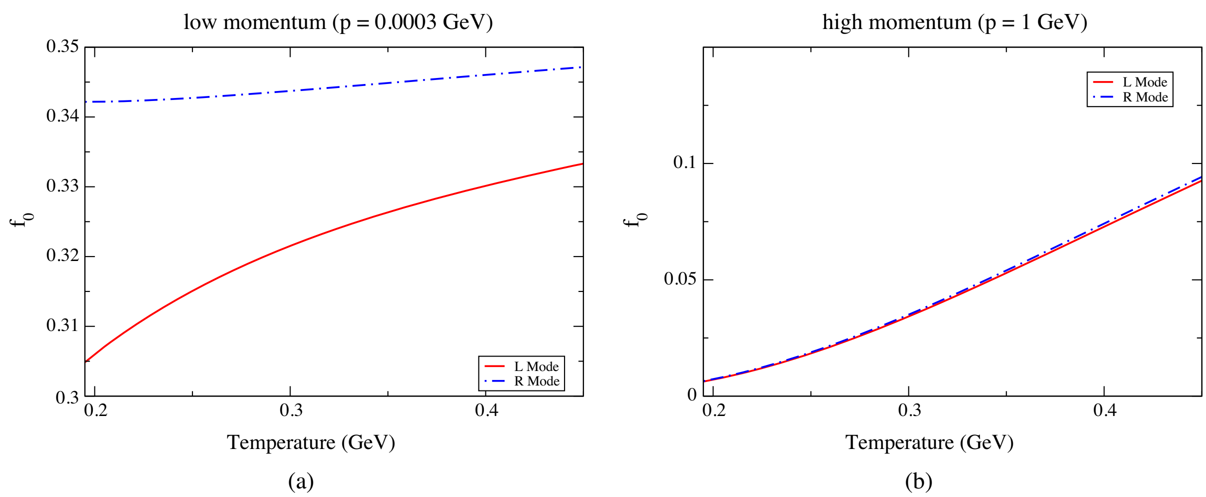

FIG. 4. Variation of distribution function of quark (f_0) in left- and right-handed mode with momentum at $T = 1.5\,T_c$ (a) and $T = 3\,T_c$ (b), where effective quark mass has been used.

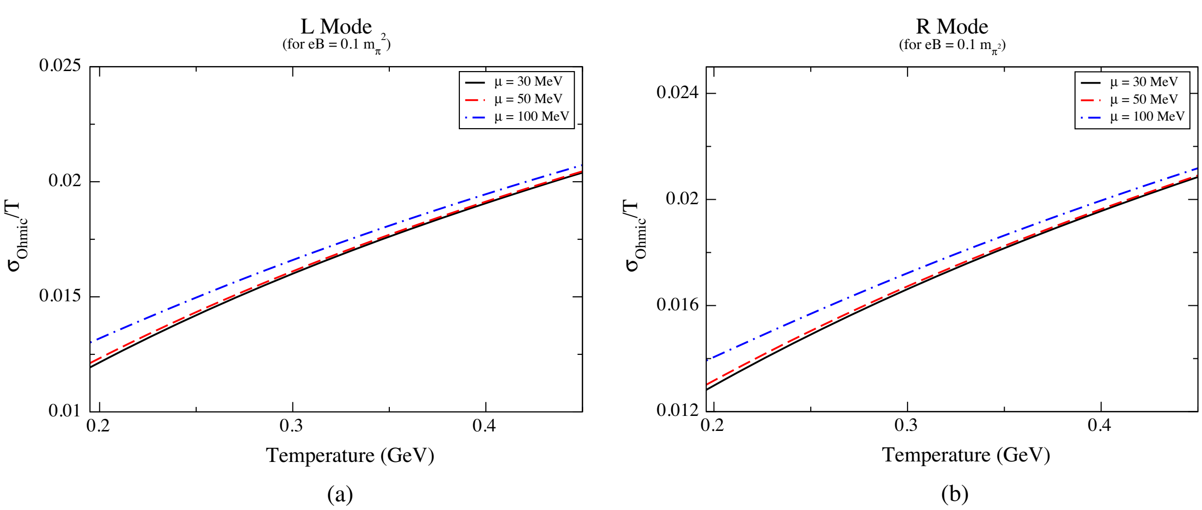

FIG. 5. Variation of $\sigma_{\mathrm{Ohmic}}/T$ for L mode (a) and R mode (b) with temperature at different fixed values of quark chemical potential.

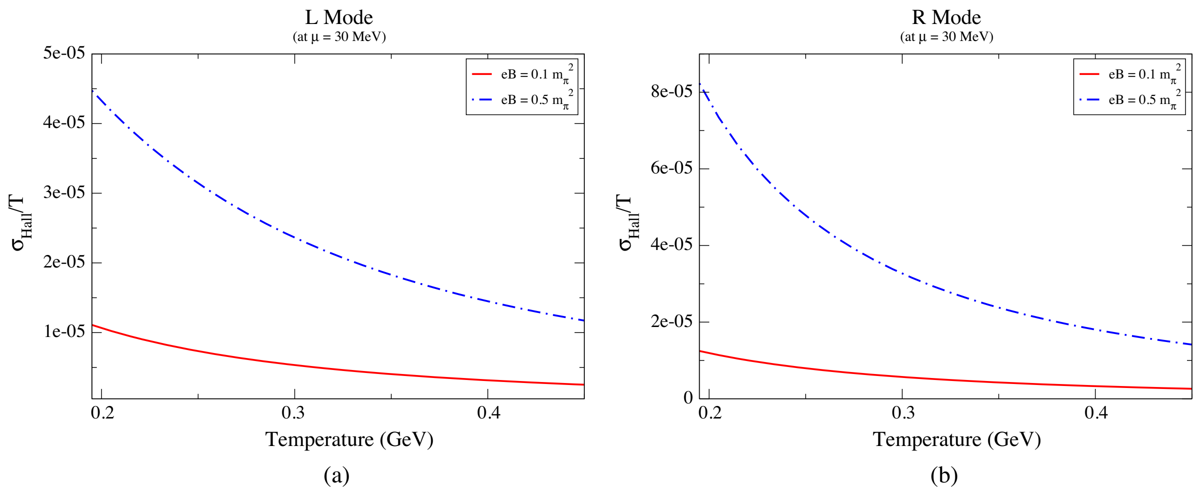

FIG. 6. Variation of σ_{Hall}/T for L mode (a) and R mode (b) with temperature at different fixed values of magnetic field.

Boltzmann factor $\exp(-\mu/T)$ increases due to the higher contribution from quarks than antiquarks. The transverse motion of charged particle under the action of Lorentz force leads to the generation of Hall current. The variation of σ_{Hall}/T with temperature for different values of magnetic field at $\mu = 30$ MeV is shown in Fig. 6 for both modes. It increases with magnetic field as σ_{Hall}/T is proportional to ω_c for the considered range of temperature, chemical potential and magnetic field. The decreasing behavior of normalized Hall conductivity with temperature is predominantly due to the factor $\omega_c\tau$ in the numerator of Eq. (72). σ_{Hall}/T for left-handed mode is relatively smaller than right-handed mode as the mass for left mode is comparatively larger than right mode. Hence, we can say that the variation of Ohmic conductivity with magnetic field is affected through the effective mass as shown in Fig. 2, where at $eB = 0$, $\sigma_{\mathrm{Ohmic}}/T$ has relatively higher magnitude. At $eB = 0$, Hall conductivity vanishes and its behavior with magnetic field is affected through the direct dependence on $q_f B$ in the numerator of Eq. (72). Similar to Ohmic conductivity, Hall conductivity also increases with quark chemical potential for L and R modes as shown in Fig. 7. At zero chemical potential, the number of quarks and antiquarks are the same and their contribution to the Hall current is the same but opposite in direction. So, the net Hall current vanishes at zero chemical potential and can be explicitly seen in Eq. (72).

B. Thermal and Hall-type thermal conductivity

Figures 8 and 9 show the variation of ratio of thermal conductivity to temperature (κ_0/T) for left- and right-handed mode with temperature at different fixed values of magnetic field and quark chemical potential respectively. At zero magnetic field, there would be no lifting of degeneracy and hence we compared κ_0/T in the absence and presence of magnetic field (with both modes). κ_0/T increases with temperature for both modes and has

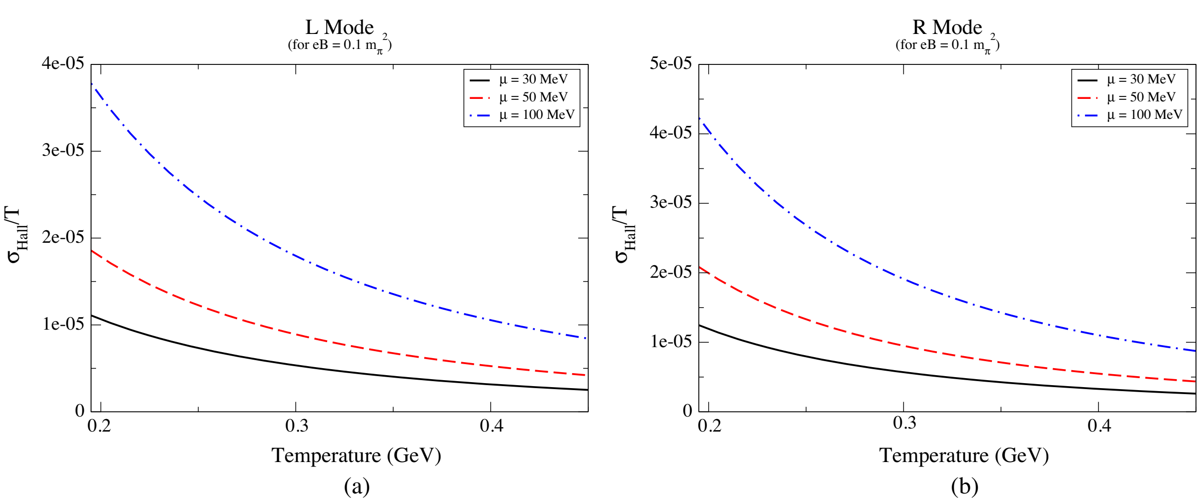

FIG. 7. Variation of σ_{Hall}/T for L mode (a) and R mode (b) with temperature at different fixed values of quark chemical potential.

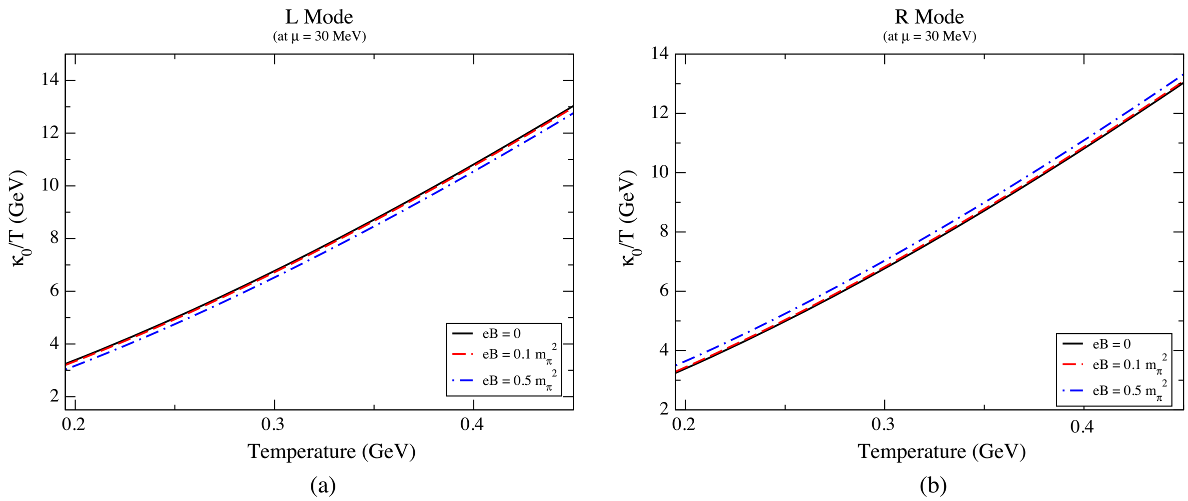

FIG. 8. Variation of κ_0/T for L mode (a) and R mode (b) with temperature at different fixed values of magnetic field.

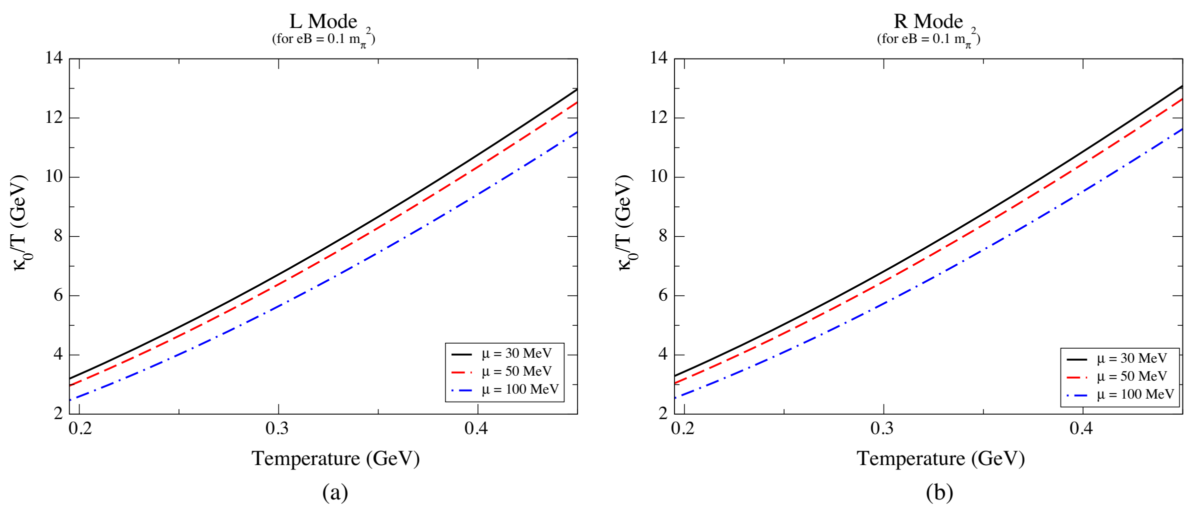

FIG. 9. Variation of κ_0/T for L mode (a) and R mode (b) with temperature at different fixed values of quark chemical potential.

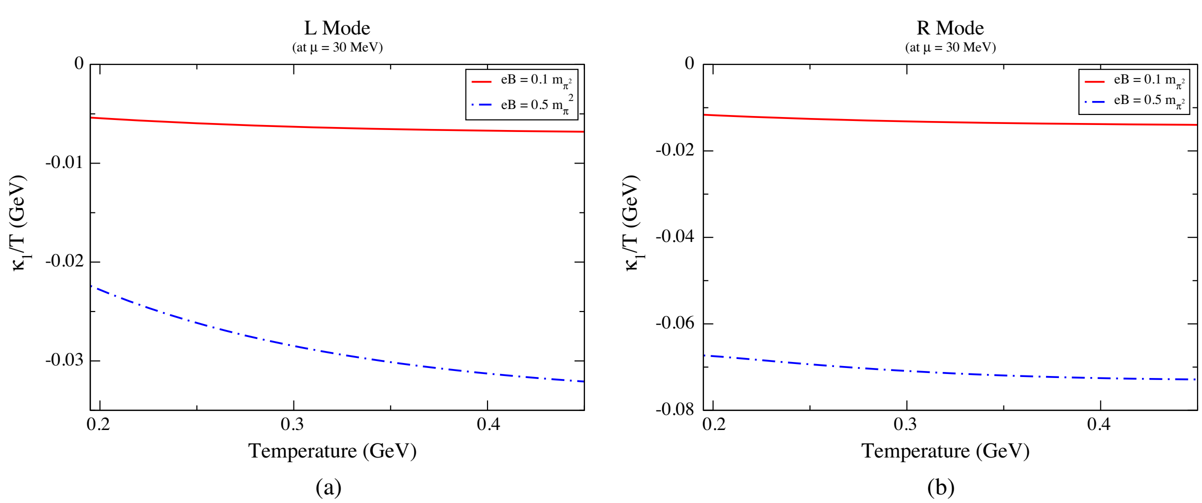

FIG. 10. Variation of κ_1/T for L mode (a) and R mode (b) with temperature at different fixed values of magnetic field.

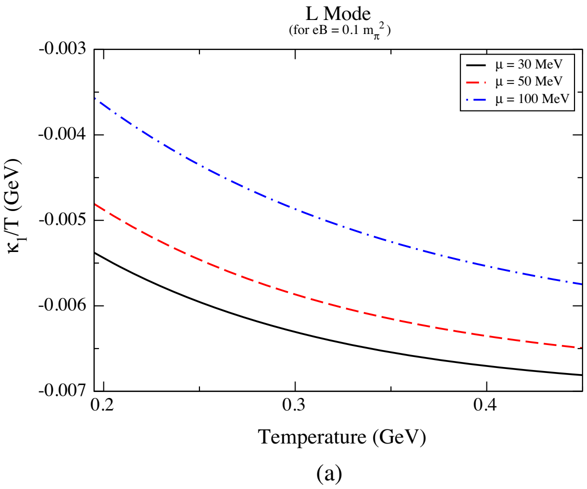

FIG. 11. Variation of κ_1/T for L mode (a) and R mode (b) with temperature at different fixed values of quark chemical potential.

approximately the same value at $\mathrm{eB} = 0.1m_\pi^2$. The increasing behavior of κ_0/T with temperature is due to the factor $(\varepsilon - h)^2$, $(\varepsilon + h)^2$ and distribution function as can be seen from Eq. (119). Further, κ_0/T for L mode decreases with magnetic field whereas for R mode it increases with magnetic field. The difference between magnitude of thermal conductivity for left- and right-handed mode is again attributed to the different effective quark mass for both modes, similar to the $\sigma_{\mathrm{Ohmic}}/T$. Since, $(\varepsilon + h)^2$ is higher in magnitude than $(\varepsilon - h)^2$ therefore $(\varepsilon + h)^2 \exp(\mu/T)$ leads to the decreasing behavior of κ_0/T with quark chemical potential for both modes. Furthermore, due to the deflected motion of particles under the action of Lorentz force, there is generation of Hall component of thermal conductivity (κ_1) in a direction perpendicular to both the magnetic field and initial thermal driving force. The variation of κ_1/T with temperature at different fixed values of magnetic field and quark chemical potential is shown in Figs. 10 and 11 respectively for both modes. Considering the absolute value of the ratio (κ_1/T), we infer that (κ_1/T) increases with temperature and magnetic field. The increasing behavior with temperature is due to the $(\varepsilon + h)^2$ factor in the numerator of Eq. (111). Moreover, the direct dependence on magnetic field leads to the amplification of Hall-type thermal conductivity with magnetic field. Further, κ_1/T decreases with quark chemical potential and will not vanish for $\mu = 0$ due to the unequal contribution from quarks and antiquarks in the same direction. We can also infer that the behavior of longitudinal thermal conductivity with magnetic field is affected through the effective quark mass for both modes whereas Hall-type thermal conductivity is affected through direct dependence on magnetic field as could be seen in Eq. (111). κ_1/T is comparatively smaller in magnitude than κ_0/T, similar to the charge transport.

C. Knudsen number

The applicability of ideal hydrodynamic requires local thermal equilibration. The degree of thermalization in fluid produced in heavy ion collision can be characterized by the dimensionless parameter which is termed Knudsen number (Ω), which is the ratio of microscopic length scale (mean-free path) to the macroscopic length scale (characteristic length scale) of the system [88]. The mean-free path (λ) is identified as $3\kappa/(\mathrm{v}C_v)$ with v and C_v as relative velocity and specific heat at constant volume respectively. Knudsen number can be recast as

$$\Omega = \frac{3\kappa}{\mathrm{v}C_v L}, \tag{120}$$

where we have taken $\mathrm{v} \simeq 1$, $L = 4$ fm. C_v is evaluated from the temperature gradient of energy density, i.e., $C_v = \partial(u_\alpha T^{\alpha\beta} u_\beta)/\partial T$. The small value of Knudsen number implies the large number of collisions which bring the system back to local equilibrium. The behavior of Ω_0 (associated to κ_0 and κ_g) and Ω_1 (associated to κ_1) with magnetic field is found to be closely related to behavior of κ_0 and κ_1 for both modes. As we can see that effect of magnetic field on C_v is not so much pronounced as shown in Figs. 12(a) and 12(b). Ω_0 decreases with magnetic field for L mode whereas increases with magnetic field for R mode as shown in Fig. 13, similar to the κ_0/T. Moreover, Ω_1 shows the increasing trend with magnetic field as shown in Fig. 14, similar to the trends followed by κ_1/T (taking the absolute value of κ_1). Knudsen number (Ω_0 and Ω_1) is found to be less than unity for both modes in the presence of weak magnetic field at $\mu = 30$ MeV, thus it ensures the system to be in thermal equilibrium.

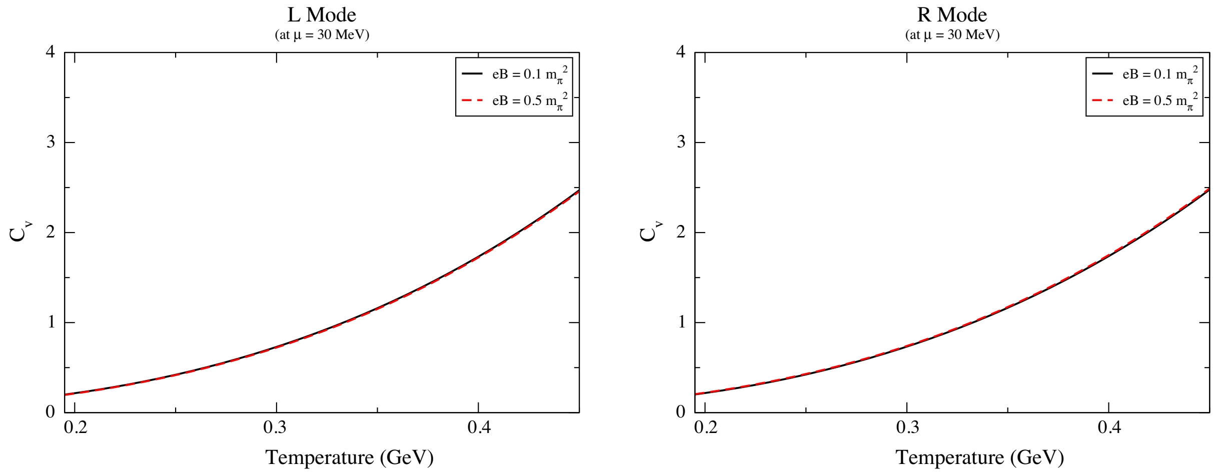

(a) (b)

FIG. 12. Variation C_v for L mode (a) and R mode (b) with temperature where effective quark mass has been used for both modes.

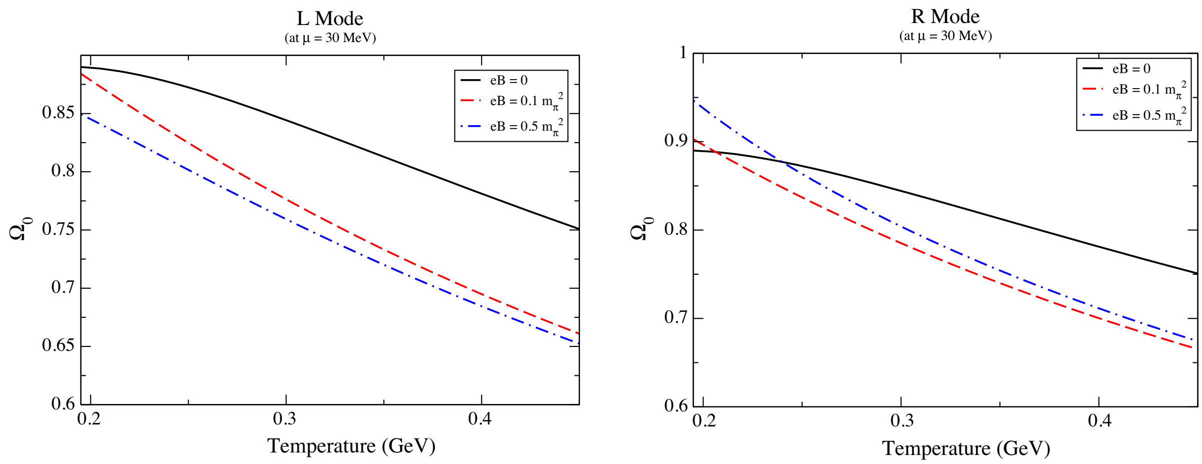

(a) (b)

FIG. 13. Variation of Knudsen number (Ω_0) for L mode (a) and R mode (b) with temperature at different fixed values of magnetic field.

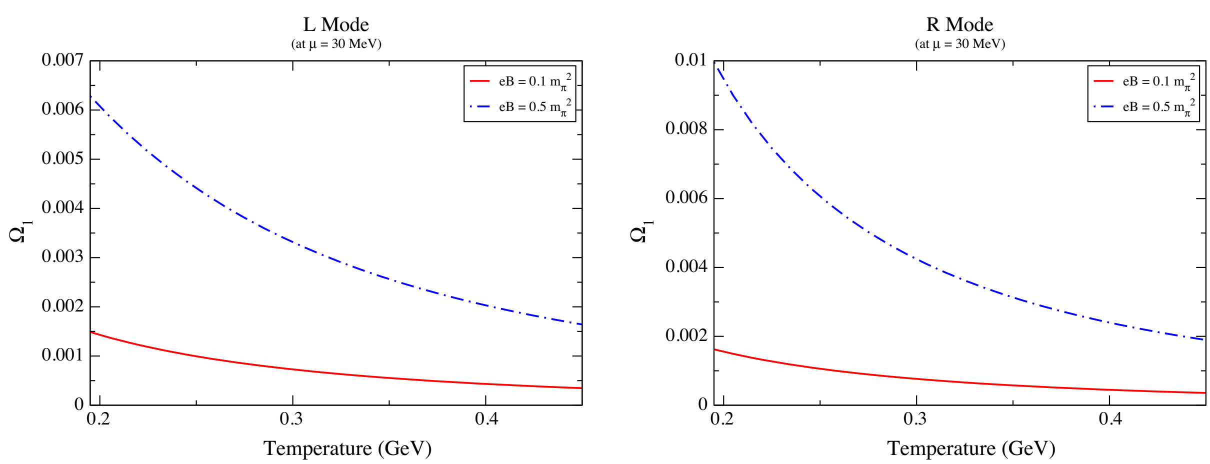

(a) (b)

FIG. 14. Variation of Knudsen number (Ω_1) for L mode (a) and R mode (b) with temperature at different fixed values of magnetic field.

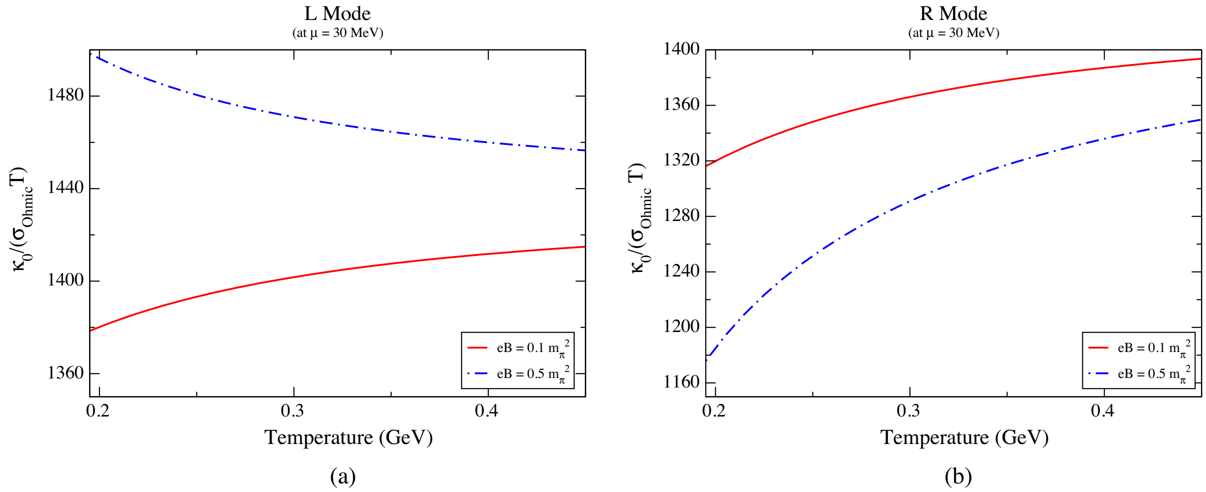

FIG. 15. Variation of Lorenz number for L mode (a) and R mode (b) with temperature at different fixed values of magnetic field.

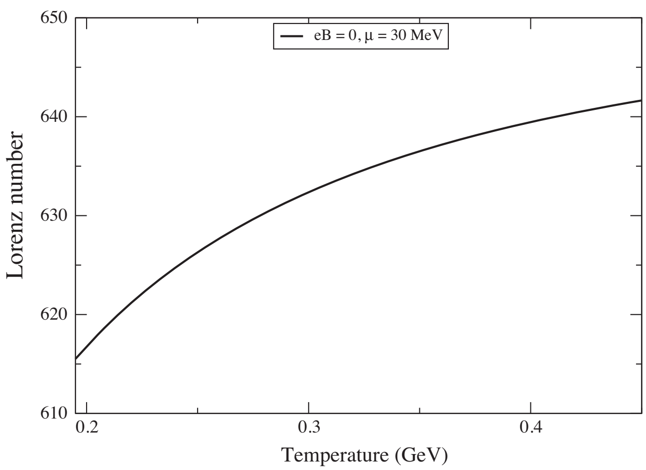

FIG. 16. Variation of Lorenz number with temperature for zero magnetic field at finite quark chemical potential.

D. Wiedemann-Franz law

The interplay between charge and heat transport coefficients can be understood via Wiedemann-Franz law. The temperature behavior of Lorenz number ($\kappa_0/\sigma_{\mathrm{Ohmic}}T$) (for L and R modes) and Hall-Lorenz number ($\kappa_1/\sigma_{\mathrm{Hall}}T$) (for L and R modes) for eB $= 0.1\ m_\pi^2$, $0.5\ m_\pi^2$ at $\mu = 30$ MeV is plotted in Figs. 15 and 17. Lorenz number in the absence of magnetic field at finite chemical potential is shown in Fig. 16. Since Lorenz and Hall-Lorenz number is larger than unity, it implies that the effect of thermal transport coefficient is more pronounced than charge transport coefficient, hence suggesting that hot QCD matter is a good conductor of heat than charge. It is evident that Lorenz and Hall Lorenz number is not constant with temperature. Lorenz number for L mode increases with magnetic field whereas for R mode decreases with magnetic field. For L mode, Lorenz number shows the increasing trend with temperature for $eB = 0.1 m_\pi^2$ whereas

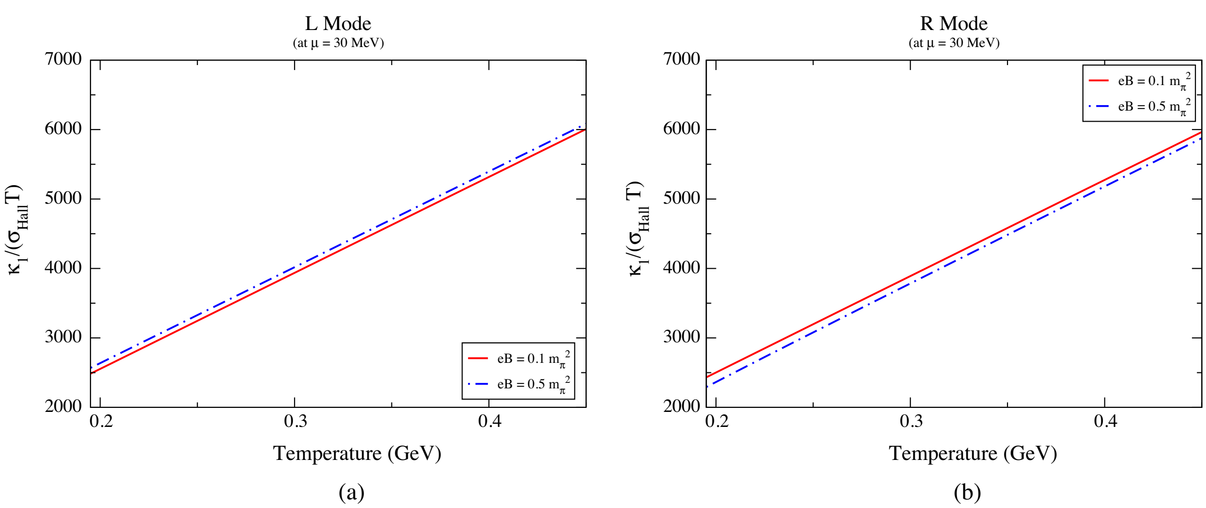

FIG. 17. Variation of Hall Lorenz number for L mode (a) and R mode (b) with temperature at different fixed values of magnetic field.

with further increase the magnetic field it starts decreasing with temperature. This opposite behavior with temperature is due to the difference in the increment of the ratio $(\kappa_0/\sigma_{\text{Ohmic}})$ at $eB = 0.1m_\pi^2, 0.5m_\pi^2$. Hall Lorenz number for L mode increases with magnetic field, whereas that for R mode decreases with magnetic field similar to the previous case as shown in Fig. 15. It increases with temperature for both modes. Here, the behavior of Lorenz number is found to be in contrast to the case of metals where it is roughly the same in the Drude model at temperatures 273 and 373 K [38]. Therefore, violation of Wiedemann-Franz law is observed.

VI. CONCLUSION

In this work, we have studied the charge and heat transport coefficients in hot QCD matter in the presence of weak magnetic field at finite chemical potential, where interactions have been incorporated through effective masses using quasiparticle description. In weak magnetic field, we have found that the left- and right-handed chiral modes of quarks get separated due to difference in their mass and become nondegenerate contrary to the strong magnetic field case. Another consequence of weak magnetic field also came into light in transport phenomena as generation of Hall effect. Transport coefficients adopt the tensorial structure where we get the nonvanishing transverse responses. The diagonal elements of tensor structure of transport coefficients give longitudinal conductivity whereas off-diagonal elements represent their Hall counterparts. We have calculated the transport coefficients using the effective mass of quarks for left- (L) and right-handed (R) chiral modes separately and studied the effect of magnetic field and quark chemical potential on transport coefficients for both modes. We studied the variation of σ_{Ohmic}/T and σ_{Hall}/T for L and R modes at different values of magnetic field and quark chemical potential with temperature. σ_{Ohmic}/T for L mode decreases with magnetic field whereas it increases with magnetic field for R mode. The opposite behavior with magnetic field for L and R modes in Ohmic conductivity is due to different values of effective quark mass for both modes. On the other hand, σ_{Hall}/T for both modes increases with magnetic field. This is due to direct dependence of magnetic field on Hall conductivity. Additionally, both conductivities for L and R modes positively amplify with quark chemical potential. Hall conductivity vanishes at zero quark chemical potential due to equal and opposite contribution of quarks and antiquarks. Analogous to Ohmic and Hall conductivity, we have studied the thermal and Hall-type thermal conductivity for both modes. Since gluons are not affected by magnetic field therefore thermal conductivity due to gluons is incorporated in longitudinal thermal conductivity. The Hall-type thermal conductivity is the manifestation of transverse temperature gradient under the action of Lorentz force. κ_0/T for L and R modes shows mutually opposite behavior with magnetic field which is again due to the different effective quark masses for left- and right-handed mode. κ_1/T increases with magnetic field for both modes similar to the Hall conductivity in charge transport. Both conductivities record a drop in their values with increasing quark chemical potential. Moreover, κ_1 does not vanish at zero quark chemical potential due to the unequal contribution from quarks and antiquarks in the same direction. In application of the aforementioned conductivities, we have investigated the equilibrium property through Knudsen number (Ω_0 and Ω_1) where it is found to be less than unity ensuring the system to be in thermal equilibrium. The variation of Knudsen number with magnetic field is found to be closely related to the thermal and Hall-type thermal conductivity, as the specific heat at constant volume does not show significant change with magnetic field. Further, the relative behavior of charge and heat transport coefficients has been studied via Wiedemann-Franz law where Lorenz and Hall Lorenz number are found to be greater than unity, hence depicting that hot QCD matter is a good conductor of heat. Moreover, Lorenz and Hall Lorenz number increases with magnetic field for L mode and decreases with magnetic field for R mode. Lorenz number for L mode (at $\text{eB} = 0.1\text{m}_\pi^2$) and for R mode (at $\text{eB} = 0.1\text{m}_\pi^2$, 0.5m_π^2) increases with temperature. As we further increase the magnetic field, Lorenz number for L mode shows a decreasing trend with temperature. So, Lorenz and Hall Lorenz number are not constant with temperature, thereby violating the Wiedemann-Franz law.

ACKNOWLEDGMENTS

P. P. would like to acknowledge Debarshi Dey and Salman Ahamad Khan for useful discussions.

APPENDIX: CALCULATION OF STRUCTURE FUNCTIONS

Here, we will show the computation of structure functions from Eq. (18) to (21) in one-loop order for hot and weakly magnetized medium under hard thermal loop (HTL) approximation. Since trace of odd number of gamma matrices is zero, Eq. (18) can be written as

$$\mathcal{A} = \frac{1}{4}\frac{\text{Tr}(\Sigma_0 \not{P}) - (P.u)\text{Tr}(\Sigma_0 \not{u})}{(P.u)^2 - P^2}, \tag{A1}$$

where

$$\Sigma_0 = g^2 C_F T \sum_n \int \frac{d^3k}{(2\pi)^3} \gamma_\mu \frac{\not{K}}{K^2 - m_f^2} \gamma^\mu \frac{1}{(P-K)^2}. \tag{A2}$$

Using the following two traces,

$$\text{Tr}[\gamma_\mu \not{K} \gamma^\mu \not{P}] = -8K.P, \tag{A3}$$

$$\mathrm{Tr}[\gamma_\mu \not{K} \gamma^\mu \not{u}] = -8K.u, \tag{A4}$$

we obtain

$$\mathcal{A}(P) = \frac{1}{4|\mathbf{p}|^2} g^2 C_F [I_1(P) + I_2(P)], \tag{A5}$$

where $(P.u)^2 - P^2 = |\mathbf{p}|^2$. We will use the frequency sum to evaluate $I_1(P)$ and $I_2(P)$ with $k_0 = i\omega_n$, $p_0 = i\omega$, $E_1 = \sqrt{k^2 + m_{f0}^2}$ and $E_2 = \sqrt{(p-k)^2}$. The frequency sum for the fermion-boson case is [68]

$$T\sum_n \tilde{\Delta}_{s1}(i\omega_n, E_1)\Delta_{s2}(i(\omega-\omega_n), E_2) = \sum_{s1,s2=\pm1} -\frac{s_1 s_2}{4E_1E_2}\frac{(1-\tilde{f}(s_1E_1) + f(s_2E_2))}{i\omega - s_1E_1 - s_2E_2}. \tag{A6}$$

The leading T^2 behavior will come from $s_1 = -s_2 = 1$ with $E_1 \approx k$ and $E_2 = |\mathbf{p} - \mathbf{k}|$. Defining lightlike four-vector $\hat{K} = (-i, \hat{\mathbf{k}})$ and $\hat{K}' = (-i, -\hat{\mathbf{k}})$, we have

$$i\omega + E_1 - E_2 \simeq i\omega + \mathbf{p}.\hat{\mathbf{k}} = P.\hat{K}, \tag{A7}$$

$$i\omega - E_1 + E_2 \simeq i\omega - \mathbf{p}.\hat{\mathbf{k}} = P.\hat{K}', \tag{A8}$$

and using the angular integration under HTL approximation,

$$\int \frac{d\Omega}{4\pi}\frac{\hat{K}.u}{P.\hat{K}} = \frac{1}{|\mathbf{p}|} Q_0\left(\frac{p_0}{|\mathbf{p}|}\right), \tag{A9}$$

we get

$$\mathcal{A}(p_0, |\mathbf{p}|) = \frac{m_{th}^2}{|\mathbf{p}|^2} Q_1\left(\frac{p_0}{|\mathbf{p}|}\right). \tag{A10}$$

Similarly, structure function $\mathcal{B}$ can be evaluated as

$$\mathcal{B}(p_0, |\mathbf{p}|) = -\frac{m_{th}^2}{|\mathbf{p}|^2}\left[\frac{p_0}{|\mathbf{p}|} Q_1\left(\frac{p_0}{|\mathbf{p}|}\right) - Q_0\left(\frac{p_0}{|\mathbf{p}|}\right)\right]. \tag{A11}$$

Using Eq. (16) in (20) and (21), where the contribution from Σ_0 vanishes due to the trace of the odd number of gamma matrices and we get the nonvanishing contribution form Σ_1 only, and hence we get

$$\mathcal{C}(p_0, |\mathbf{p}|) = -\frac{1}{4}\mathrm{Tr}(\gamma_5 \Sigma_1 \not{u}), \tag{A12}$$

$$\mathcal{D}(p_0, |\mathbf{p}|) = \frac{1}{4}\mathrm{Tr}(\gamma_5 \Sigma_1 \not{b}). \tag{A13}$$

Using the following two traces,

$$\mathrm{Tr}[\gamma_5\gamma_\mu\gamma_5[(K.b)\not{u} - (K.u)\not{b}]\gamma^\mu \not{u}] = 8(K.b), \tag{A14}$$

$$\mathrm{Tr}[\gamma_5\gamma_\mu\gamma_5[(K.b)\not{u} - (K.u)\not{b}]\gamma^\mu \not{b}] = 8(K.u), \tag{A15}$$

we obtain

$$\mathcal{C} = \frac{g^2 C_F |q_f B|}{4} T\sum_n \int \frac{d^3k}{(2\pi)^3}\frac{8(K.b)}{(K^2 - m_{f0}^2)^2 (P-K)^2}, \tag{A16}$$

$$\mathcal{D} = -\frac{g^2 C_F |q_f B|}{4} T\sum_n \int \frac{d^3k}{(2\pi)^3}\frac{8(K.u)}{(K^2 - m_{f0}^2)^2 (P-K)^2}, \tag{A17}$$

which in turn requires the calculation of frequency sum [89]

$$Y = T\sum_n \Delta_F^2(K)\Delta_B(P-K), = \left(\frac{-\partial}{\partial m_{f0}^2}\right) T\sum_n \Delta_F(K)\Delta_B(P-K), \tag{A18}$$

where

$$T\sum_n \Delta_F(K)\Delta_B(P-K) = \sum_{s1,s2=\pm1} -\frac{s_1 s_2}{4E_1E_2}\frac{(1-\tilde{f}(s_1E_1) + f(s_2E_2))}{i\omega - s_1E_1 - s_2E_2}. \tag{A19}$$

For $s_1 = -s_2 = 1$, we get

$$\mathcal{C} = \frac{4g^2 C_F |q_f B|}{16\pi^2}\left(\frac{\pi T}{2m_{f0}} - \ln 2 + \frac{7\mu^2\zeta(3)}{8\pi^2 T^2}\right)\left[\frac{-p_z}{|\mathbf{p}|^2} Q_1\left(\frac{p_0}{|\mathbf{p}|}\right)\right], \tag{A20}$$

$$\mathcal{D} = -\frac{4g^2 C_F |q_f B|}{16\pi^2}\left(\frac{\pi T}{2m_{f0}} - \ln 2 + \frac{7\mu^2\zeta(3)}{8\pi^2 T^2}\right)\left[\frac{1}{|\mathbf{p}|} Q_0\left(\frac{p_0}{|\mathbf{p}|}\right)\right]. \tag{A21}$$

[1] M. Gyulassy and L. McLerran, Nucl. Phys. **A750**, 30 (2005).
[2] V. V. Skokov, A. Yu. Illarionov, and V. D. Toneev, Int. J. Mod. Phys. A **24**, 5925 (2009).
[3] D. E. Kharzeev, L. D. McLerran, and H. J. Warringa, Nucl. Phys. **A803**, 227 (2008).
[4] K. Fukushima, D. E. Kharzeev, and H. J. Warringa, Phys. Rev. Lett. **104**, 212001 (2010).
[5] K. Tuchin, Phys. Rev. C **88**, 024911 (2013).
[6] K. Tuchin, Phys. Rev. C **93**, 014905 (2016).
[7] L. McLerran and V. Skokov, Nucl. Phys. **A929**, 184 (2014).
[8] E. Stewart and K. Tuchin, Phys. Rev. C **97**, 044906 (2018).
[9] A. Das, S. S. Dave, P. S. Saumia, and A. M. Srivastava, Phys. Rev. C **96**, 034902 (2017).
[10] K. Tuchin, Phys. Rev. C **83**, 017901 (2011).
[11] M. Greif, C. Greiner, and G. S. Denicol, Phys. Rev. D **93**, 096012 (2016).
[12] M. Greif, I. Bouras, C. Greiner, and Z. Xu, Phys. Rev. D **90**, 094014 (2014).
[13] A. Puglisi, S. Plumari, and V. Greco, Phys. Lett. B **751**, 326 (2015).
[14] A. Puglisi, S. Plumari, and V. Greco, Phys. Rev. D **90**, 114009 (2014).
[15] W. Cassing, O. Linnyk, T. Steinert, and V. Ozvenchuk, Phys. Rev. Lett. **110**, 182301 (2013).
[16] T. Steinert and W. Cassing, Phys. Rev. C **89**, 035203 (2014).
[17] S. Rath and B. K. Patra, Phys. Rev. D **100**, 016009 (2019).
[18] D. Dey and B. K. Patra, Phys. Rev. D **102**, 096011 (2020).
[19] S. Rath and B. K. Patra, J. High Energy Phys. 12 (2017) 098.
[20] B. Karmakar, R. Ghosh, A. Bandyopadhyay, N. Haque, and M. G. Mustafa, Phys. Rev. D **99**, 094002 (2019).
[21] K. Tuchin, Phys. Rev. C **88**, 024910 (2013).
[22] A. Peshier and M. H. Thoma, Phys. Rev. Lett. **84**, 841 (2000).
[23] K. A. Mamo, J. High Energy Phys. 08 (2013) 083.
[24] U. Heinz and R. Snellings, Annu. Rev. Nucl. Part. Sci. **63**, 123 (2013).
[25] B. Schenke, S. Jeon, and C. Gale, Phys. Rev. C **82**, 014903 (2010).
[26] H. Niemi, G. S. Denicol, P. Huovinen, E. Molnar, and D. H. Rischke, Phys. Rev. Lett. **106**, 212302 (2011).
[27] P. K. Kovtun, D. T. Son, and A. O. Starinets, Phys. Rev. Lett. **94**, 111601 (2005).
[28] P. Romatschke and U. Romatschke, Phys. Rev. Lett. **99**, 172301 (2007).
[29] D. Teaney, J. Lauret, and E. V. Shuryak, Phys. Rev. Lett. **86**, 4783 (2001).
[30] P. Huovinen, P. F. Kolb, U. Heinz, P. V. Ruuskanen, and S. A. Voloshin, Phys. Lett. B **503**, 58 (2001).
[31] R. Baier, P. Romatschke, and U. A. Wiedemann, Phys. Rev. C **73**, 064903 (2006).
[32] U. Heinz, H. Song, and A. K. Chaudhuri, Phys. Rev. C **73**, 034904 (2006).
[33] G. S. Denicol, H. Niemi, I. Bouras, E. Molnár, Z. Xu, D. H. Rischke, and C. Greiner, Phys. Rev. D **89**, 074005 (2014).
[34] S. Ghosh, Int. J. Mod. Phys. E **24**, 1550058 (2015).
[35] G. Kadam, H. Mishra, and L. Thakur, Phys. Rev. D **98**, 114001 (2018).
[36] K. Fukushima, D. E. Kharzeev, and H. J. Warringa, Phys. Rev. D **78**, 074033 (2008).
[37] K. Haglin, C. Gale, and V. Emel'yanov, Phys. Rev. D **47**, 973 (1993).
[38] Neil W. Ashcroft and N. David Mermin, *Solid State Physics* (Saunders College Publishing, Philadelphia, 1976).
[39] A. Principi and G. Vignale, Phys. Rev. Lett. **115**, 056603 (2015).
[40] R. W. Hill, C. Proust, L. Taillefer, P. Fournier, and R. L. Greene, Nature (London) **414**, 711 (2001).
[41] A. Garg, D. Rasch, E. Shimshoni, and A. Rosch, Phys. Rev. Lett. **103**, 096402 (2009).
[42] S. Mitra and V. Chandra, Phys. Rev. D **96**, 094003 (2017).
[43] R. Rath, S. Tripathy, B. Chatterjee, R. Sahoo, S. K. Tiwari, and A. Nath, Eur. Phys. J. A **55**, 125 (2019).
[44] K. Fukushima, K. Hattori, H.-Ung Yee, and Y. Yin, Phys. Rev. D **93**, 074028 (2016).
[45] R. Marty, E. Bratkovskaya, W. Cassing, J. Aichelin, and H. Berrehrah, Phys. Rev. C **88**, 045204 (2013).
[46] R. Lang, N. Kaiser, and W. Weise, Eur. Phys. J. A **51**, 127 (2015).
[47] S. Ghosh, F. E. Serna, A. Abhishek, G. Krein, and H. Mishra, Phys. Rev. D **99**, 014004 (2019).
[48] A. Wiranata and M. Prakash, Phys. Rev. C **85**, 054908 (2012).
[49] S. Plumari, A. Puglisi, F. Scardina, and V. Greco, Phys. Rev. C **86**, 054902 (2012).
[50] S. Mitra and V. Chandra, Phys. Rev. D **94**, 034025 (2016).
[51] S. Ghosh, Int. J. Mod. Phys. A **29**, 1450054 (2014).
[52] A. Harutyunyan, D. H. Rischke, and A. Sedrakian, Phys. Rev. D **95**, 114021 (2017).
[53] N. Demir and A. Wiranata, J. Phys. Conf. Ser. **535**, 012018 (2014).
[54] S. Satapathy, S. Ghosh, and S. Ghosh, Phys. Rev. D **104**, 056030 (2021).
[55] M. Kurian and V. Chandra, Phys. Rev. D **97**, 116008 (2018).
[56] M. Kurian and V. Chandra, Phys. Rev. D **96**, 114026 (2017).
[57] M. Kurian, Phys. Rev. D **102**, 014041 (2020).
[58] K. K. Gowthama, M. Kurian, and V. Chandra, Phys. Rev. D **103**, 074017 (2021).
[59] S. Gupta, Phys. Lett. B **597**, 57 (2004).
[60] G. Aarts, C. Allton, A. Amato, P. Giudice, S. Hands, and J.-I. Skullerud, J. High Energy Phys. 02 (2015) 186.
[61] H.-T. Ding, O. Kaczmarek, and F. Meyer, Phys. Rev. D **94**, 034504 (2016).
[62] S. Rath and B. K. Patra, Eur. Phys. J. C **80**, 747 (2020).
[63] S. A. Khan and B. K. Patra, Phys. Rev. D **104**, 054024 (2021).
[64] A. Das, H. Mishra, and R. K. Mohapatra, Phys. Rev. D **101**, 034027 (2020).
[65] L. Thakur and P. K. Srivastava, Phys. Rev. D **100**, 076016 (2019).
[66] A. Das, A. Bandyopadhyay, P. K. Roy, and M. G. Mustafa, Phys. Rev. D **97**, 034024 (2018).
[67] H. A. Weldon, Phys. Rev. D **26**, 2789 (1982).
[68] M. Le Bellac, *Thermal Field Theory* (Cambridge University Press, Cambridge, England, 1996).
[69] A. Ayala, C. A. Dominguez, S. Hernandez-Ortiz, L. A. Hernandez, M. Loewe, D. Manreza Paret, and R. Zamora, Phys. Rev. D **98**, 031501(R) (2018).

[70] J.-P. Blaizot and E. Iancu, Phys. Rep. **359**, 355 (2002).
[71] V. M. Bannur, J. High Energy Phys. 09 (2007) 046.
[72] J. Schwinger, Phys. Rev. **82**, 664 (1951).
[73] T.-K. Chyi, C.-W. Hwang, W. F. Kao, G.-L. Lin, K.-W. Ng, and J.-J. Tseng, Phys. Rev. D **62**, 105014 (2000).
[74] A. Bandyopadhyay, B. Karmakar, N. Haque, and M. G. Mustafa, Phys. Rev. D **100**, 034031 (2019).
[75] L. D. Landau and E. M. Lifshitz, *Course of Theoretical Physics, Volume 10, Physical Kinetics* (Pergamon International Library, New York, 1981).
[76] B. Feng, Phys. Rev. D **96**, 036009 (2017).
[77] A. Hosoya and K. Kajantie, Nucl. Phys. **B250**, 666 (1985).
[78] H. Berrehrah, E. Bratkovskaya, W. Cassing, P. B. Gossiaux, J. Aichelin, and M. Bleicher, Phys. Rev. C **89**, 054901 (2014).
[79] M. Cheng *et al.*, Phys. Rev. D **77**, 014511 (2008).
[80] C. Schmidt *et al.*, Nucl. Phys. **A820**, 41C (2009).
[81] L. L. Zhu and C. B. Yang, Nucl. Phys. **A831**, 49 (2009).
[82] S. Groot, W. van Leeuwen, and Ch. G. van Weert, *Relativistic Kinetic Theory* (North-Holland Publishing Company, New York, 1980).
[83] L. D. Landau and E. M. Lifshitz, *Course of Theoretical Physics, Volume 6, Fluid Mechanics* (Pergamon Books Ltd., New York, 1987).
[84] M. Greif, F. Reining, I. Bouras, G. S. Denicol, Z. Xu, and C. Greiner, Phys. Rev. E **87**, 033019 (2013).
[85] W. Israel and J. M. Stewart, Ann. Phys. (N.Y.) **118**, 341 (1979).
[86] A. Haug, *Theoretical Solid State Physics, Volume 2* (Pergamon Press Ltd., New York, 1972).
[87] Charles R. Whitsett, J. Appl. Phys. **32**, 2257 (1961).
[88] A. K. Chaudhuri, Phys. Rev. C **82**, 047901 (2010).
[89] A. Ayala, J. J. Cobos-Martínez, M. Loewe, M. E. Tejeda-Yeomans, and R. Zamora, Phys. Rev. D **91**, 016007 (2015).